^{40}Ar–^{39}Ar ages and isotope geochemistry of Cretaceous basalts in northern Madagascar: refining eruption ages, extent of crustal contamination and parental magmas in a flood basalt province

C. CUCCINIELLO*, L. MELLUSO*†, F. JOURDAN‡, J. J. MAHONEY§,
T. MEISEL¶ & V. MORRA*

*Dipartimento di Scienze della Terra, Universita' di Napoli Federico II, via Mezzocannone 8, 80134 Napoli, Italy
‡Western Australian Argon Isotope Facility Department of Applied Geology & JdL Centre,
Curtin University of Technology, GPO Box U1987, Perth, WA 6845, Australia
§School of Ocean and Earth Science and Technology, University of Hawaii at Manoa, Honolulu, Hawaii 96822, USA
¶General and Analytical Chemistry, Montanuniversität Leoben, Austria

Abstract – The Madagascar Cretaceous igneous province exposed in the Mahajanga basin is represented by basalt and basaltic andesite lavas. New ^{40}Ar–^{39}Ar plateau ages (92.3 ± 2.0 Ma and 91.5 ± 1.3 Ma) indicate that the magmatism in the Mahajanga basin started about 92 Ma ago. Four geochemically distinct magma types (Groups A–D) are present. Group A and C rocks have low to moderate TiO_2 (1.2–2.6 wt %), Nb (3–9 µg g^{-1}) and Zr (82–200 µg g^{-1}), and show large variations in εNd_i (+0.1 to −10.8), ^{206}Pb/^{204}Pb (15.28 to 16.33) and γ_{Os} (+11.4 to +7378). The large isotopic variations, particularly in Os, Nd and Pb isotopic compositions, are likely due to crustal contamination. The low Pb isotope ratios observed in the Group A and C rocks suggest involvement of continental crust with low µ (^{238}U/^{204}Pb). Group B and D rocks have moderate to high TiO_2 (2.2–4.9 wt %), Nb (8–24 µg g^{-1}) and Zr (120–327 µg g^{-1}). Age-corrected isotopes of Group B and D lavas show a small range in εNd_i (+1.0 to +4.0) and a wide range in γ_{Os} (+128 to +1182). Values of ^{207}Pb/^{204}Pb are within the range for Groups A and C, but the Group D ^{206}Pb/^{204}Pb (16.52–17.08) and ^{208}Pb/^{204}Pb (37.51–38.01) values are higher, indicating a different crustal contaminant. Pb isotopic values of the Group B rocks seem to reflect the isotopic features of their mantle source. The magma groups of Mahajanga display a wide range of trace element and isotopic compositions that cannot be explained only by open-system crystallization processes but, rather, by distinct mantle sources.

Keywords: ages, isotope geochemistry, Madagascar, basalts, Cretaceous.

1. Introduction

During Late Cretaceous time, extensive basaltic magmatism occurred in Madagascar. Remnants of this igneous province crop out along the rifted margin of the eastern coast, in the Mahajanga and Morondava basins of western Madagascar and directly above the Precambrian basement, and comprise lava flows, dykes, sills and intrusive complexes (Mahoney, Nicollet & Dupuy, 1991; Storey *et al.* 1995; Storey, Mahoney & Saunders, 1997; Melluso *et al.* 1997, 2001, 2002, 2003, 2005, 2009; Melluso, Morra & Fedele, 2006; Mahoney *et al.* 2008; Fig. 1a). The original pre-erosion extent of the province is difficult to estimate, although it probably exceeded 1×10^6 km² (this estimate includes the Madagascar Plateau, which flanks the south coast of Madagascar, and the Conrad Rise; Storey *et al.* 1995). The dominant rock type is tholeiitic basalt. Silicic rocks do not represent a substantial part of the eruptive stratigraphy (e.g. Melluso *et al.* 2009; Cucciniello *et al.* 2010). Only in the Volcan de l'Androy complex (southern Madagascar) are silicic rocks abundant, and

even there they are interbedded with basaltic flows (Mahoney *et al.* 2008).

Published ^{40}Ar–^{39}Ar and U–Pb ages indicate that the Madagascar Cretaceous igneous province was emplaced over a period of several million years between 92 and 84 Ma (Storey *et al.* 1995; Torsvik *et al.* 1998; Melluso *et al.* 2005; Cucciniello *et al.* 2010, 2011). In the south, the ^{40}Ar–^{39}Ar ages are mainly concentrated along the eastern coast (Mananjary and Vatomandry transects) and in the Androy area (Volcan de l'Androy complex), and range from 90 to 84 Ma (Storey *et al.* 1995; Cucciniello *et al.* 2011). In the north, the ^{40}Ar–^{39}Ar ages are mainly focused in the eastern Mahajanga basin (Bongolava–Manasamody plateau) and in the Sambava and Tamatave districts, and range from 86 to 90 Ma (Storey *et al.* 1995). U–Pb ages are few and are available for the capping rhyodacitic unit of the Mailaka lava succession and for the Analalava and Antampombato–Ambatovy intrusions, and range from 90 to 92 Ma (Torsvik *et al.* 1998; Melluso *et al.* 2005; Cucciniello *et al.* 2010). However, all available age determinations are insufficient because they do not cover the whole province, ignoring many important areas such as the western Mahajanga basin (Antanimena plateau) and the Mailaka basaltic lava

†Author for correspondence: melluso@unina.it
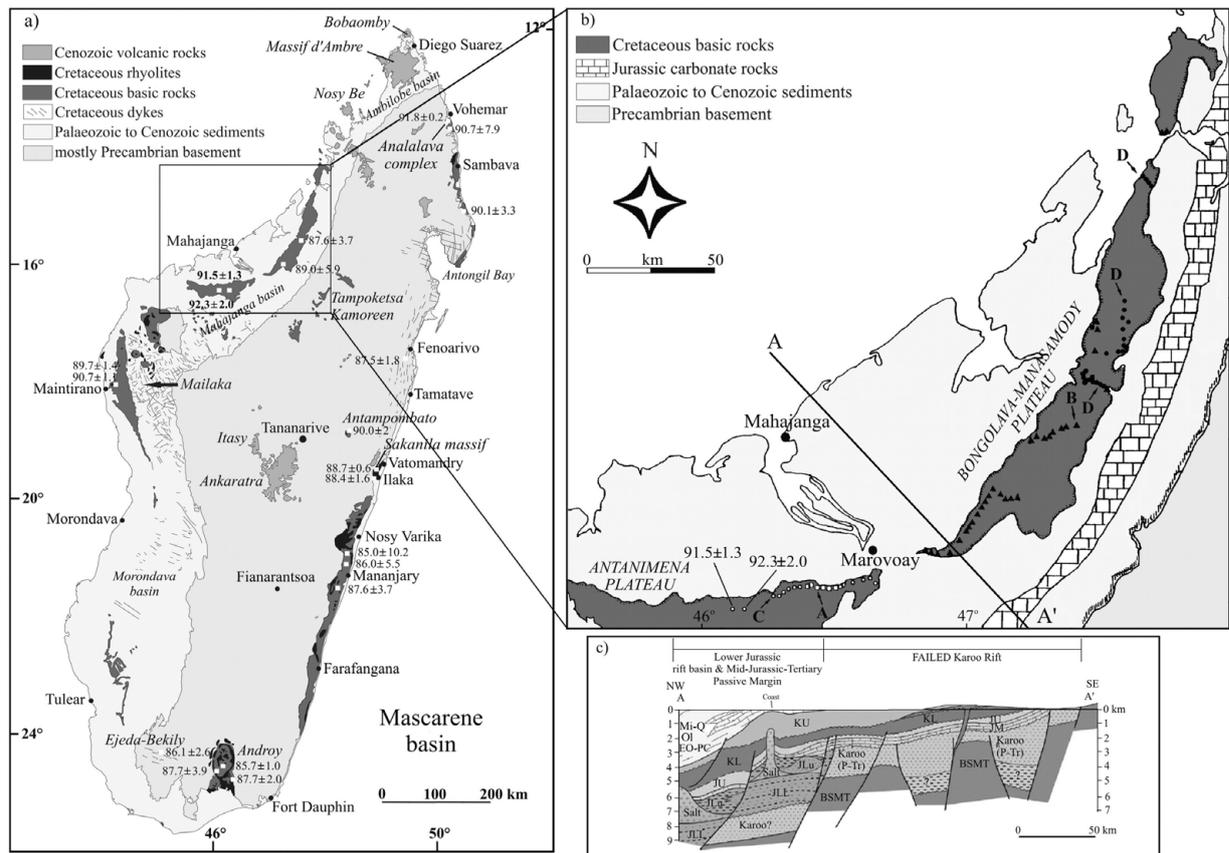
Figure 1. (a) Simplified geological map of Madagascar, showing the outcrops of Cretaceous igneous rocks (black and dark grey areas). Published ^{40}Ar–^{39}Ar and U–Pb ages that are considered to be reliable for the Madagascar Cretaceous igneous province are also indicated (± 2σ). ^{40}Ar–^{39}Ar ages have been recalculated using the new decay constants determined by Renne *et al.* (2010). New ^{40}Ar–^{39}Ar ages for the Antanimena plateau (in Ma) are in bold. (b) Sketch map of the Mahajanga basin (after Besairie, 1964) with the location of four magma groups recognized by Melluso *et al.* (1997). (c) Schematic geological cross-section of the onshore Mahajanga basin (after Banks *et al.* 2008). The basin can be divided into a Permo-Triassic failed rift filled with Karoo-related sediments (towards the east) and a Late Jurassic–Cenozoic passive margin filled with a thick succession of deposits post-Triassic (towards the west). Q – Quaternary; Mi – Miocene; Ol – Oligocene; EO–PC – Eocene–Paleocene; KU – Upper Cretaceous; KL – Lower Cretaceous; JU – Upper Jurassic; JM – Middle Jurassic; JLu – Lower Jurassic undifferentiated; JLL – Lowest Lower Jurassic; P–Tr – Permian–Triassic; BSMT – Basement.

succession. In addition, most of the previous ^{40}Ar–^{39}Ar ages are not of optimum robustness (a critical review of previous age determinations is given in Section 4) and this can affect understanding of the true duration of the Madagascar province.

An extensive study of the igneous rocks that crop out along the eastern coast (Sambava, Tamatave and Mananjary sectors) of the province was carried out by Storey, Mahoney & Saunders (1997). They identified two compositional trends (Trends I and II). Trend I appears to have been derived by mixing of normal mid-ocean-ridge-basalt (MORB)-like mantle and a Marion hotspot component, whereas Trend II is consistent with mixing of a low ^{206}Pb/^{204}Pb lithospheric-mantle-derived component with a normal-MORB-like mantle component. In addition, some high-Si, low-Ti-Nb basalts in the Mananjary district show signs of crustal contamination (Storey, Mahoney & Saunders, 1997).

Melluso *et al.* (2005) reported mineral and geochemical data for the Antampombato–Ambatovy complex and associated dyke swarm of central-eastern Madagascar. They noted that the Sr–Nd isotopic ratios for the mafic-ultramafic rocks are most similar to those of the MORB-like igneous rocks of eastern Madagascar, and suggested the existence of a component in the source of the entire Madagascar province that had a long history of relative depletion in the highly incompatible elements.

The tholeiitic rocks (from picritic basalts to rhyodacites) from the Mailaka district (Fig. 1) are depleted in high-field-strength elements (HFSE) and show a wide range in Sr–Nd–Pb isotope ratios. The transitional rocks (from picritic basalts to basalts) have incompatible element abundances and Pb, Os and Nd isotope ratios within the range of MORB. Melluso *et al.* (2001, 2003) and Cucciniello *et al.* (2010) argued that the Mailaka tholeiitic rocks were derived from a MORB-like mantle source, but contaminated by continental crust en route to the surface. In contrast, the chemical variations observed in transitional basalt lavas and dykes in this area were attributed to nearly closed-system fractional crystallization.

Detailed studies of the southern part of this province were reported by Mahoney, Nicollet & Dupuy (1991),

Dostal *et al.* (1992) and Mahoney *et al.* (2008). These authors identified: (1) tholeiitic basalts in the southeastern coastal area; (2) tholeiitic basalts and basaltic andesites in the southwestern area and in the Ejeda–Bekily dyke swarm; (3) dykes of alkaline basalts and basanites; and (4) tholeiitic and andesitic basalts (Group B1), transitional basalts (Group B2) and rhyolites (Group R1 and R2) in the Androy complex. Mahoney, Nicollet & Dupuy (1991) showed that the southwestern tholeiitic basalts were variably contaminated by ancient, low εNd and high ^{87}Sr/^{86}Sr continental material, whereas the Ejeda–Bekily alkaline rocks seem not to have been contaminated by continental material. Three different mantle sources (Marion hotspot, a N-MORB-like component and an unusual low ^{206}Pb/^{204}Pb, low-εNd source) were invoked to explain the different geochemical features observed.

The focus of this paper is on a basalt sequence exposed in the northern part of the Madagascar Cretaceous igneous province (Mahajanga basin; Fig. 1). Detailed studies of the northern Madagascar basalts were published by Melluso *et al.* (1997, 2002, 2003). They argued on the basis of trace element and Sr–Nd isotopic data that the basaltic rocks from the Antanimena plateau (Groups A and C) were derived from a MORB-like mantle source and affected by variable amounts of contamination by crustal materials, whereas the basalts from the Bongolava–Manasamody plateau (Groups B and D) were derived from long-term incompatible-element-enriched lithospheric mantle and that crustal assimilation was minor. However, the nature of the crustal contaminants and the role of the Marion hotspot (heat source to the lithosphere or magma source) are not well understood. The Pb isotope system, when combined with other isotopic systems, can help significantly to identify crustal components in mantle-derived magmas because U, Th and Pb are more enriched in the continental crust than in the mantle and fractionation of the U/Pb and Th/Pb ratios during crustal processes (e.g. metamorphism, hydrothermal alteration) can be large (e.g. Kramers & Tolstikhin, 1997).

The Re–Os isotopic system is another potentially powerful tool for tracing the crustal components in mantle-derived magmas. The different behaviour of Re and Os during melting or fractional crystallization (Os behaves compatibly during partial melting and fractional crystallization, whereas Re is a mildly incompatible element) yields, over time, two clearly distinct types of Os isotope signatures in mantle and crustal reservoirs (e.g. Shirey & Walker, 1998; Saal *et al.* 1998). Significant differences in Re and Os concentration between the continental crust and the mantle make hot mantle-derived magmas ultra-sensitive to crustal contamination. In addition, the Re–Os system may be used to distinguish between different mantle components involved in the genesis of basaltic magmas (e.g. Xu *et al.* 2007; Dale *et al.* 2009).

In this paper we present new high-precision ^{40}Ar–^{39}Ar ages and Pb–Os isotope data to assess the petrogenesis of each magma type and evaluate the role of crustal contamination. Details of analytical methods are given in Appendix 1. In addition, we give a brief outline of a scenario for the origin of the Mahajanga flood basalt sequence.

2. Geological setting

During Proterozoic and early Palaeozoic times, Madagascar was situated within the East African Orogen (EAO; e.g. Stern, 1994). From Permo-Carboniferous times onwards, crustal extension in the centre of Gondwana determined the formation of three major sedimentary basins along the western margin of Madagascar (Morondava, Mahajanga and Ambilobe basins; Fig.1a). The Mahajanga basin is the second largest basin of Madagascar and extends for almost 400 km along the northwestern coast (Fig. 1b). It is filled by a thick sequence of sediments of the Karoo Supergroup (Besaire & Collignon, 1972; Razafindrazaka *et al.* 1999; Banks *et al.* 2008; Fig. 1b, c). The sediments overlie the basement, which is composed of deformed and metamorphosed Precambrian granitoids and subordinate mafic-ultramafic rocks, ranging in age between 3.2 Ga and ≈ 550 Ma (e.g. Tucker *et al.* 1999; Collins & Windley, 2002; De Waele *et al.* 2011). The sedimentary rocks of the Karoo Supergroup are subdivided into the Sakoa (Late Carboniferous/Early Permian), Sakamena (Late Permian/Early Triassic) and Isalo (Late Triassic/Early Jurassic) groups. The Sakoa group is absent in the Mahajanga basin. The Sakamena and Isalo groups are composed of continental sediments with minor marine deposits, whereas the post-Karoo sequences (from Middle Jurassic to present) are mainly marine (Fig. 1b, c). During Late Cretaceous time, a sequence (up to 200 m remaining thickness) of flood basalts covered the Permo-Triassic to Lower Cretaceous sedimentary succession. The basalt flows crop out in a wide area of the basin (forming the Antanimena and Bongolava–Manasamody plateaus) and gently dip northwards (≈ 1°). Determination of a clear stratigraphic order for these basalts is precluded because of flat morphology and generally poor exposure of the outcrops. Melluso *et al.* (2002) argued that the Group D basalts partially overlap the Group B basalts in the upper sequence, because no Group D basalts have been found in the Bongolava area, whereas Group B basalts were observed at the end of the sequence in some parts of the Manasamody plateau (Fig. 1b). A dyke swarm is present south of the Antanimena plateau. The chemical and isotopic composition of the dykes is identical to that of the basaltic flows.

Remnants of Cretaceous lava flows also crop out in the Tampoketsa Kamoreen area (about 150 km southeast of Mahajanga; Fig. 1a). The lava flows lie directly above mafic granulites, amphibole gneisses and muscovite-bearing leucogneisses of the Precambrian basement (Melluso *et al.* 2003; De Waele *et al.* 2011).
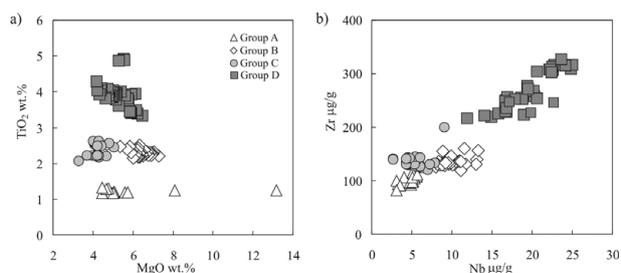
Figure 2. Variations in TiO_2 v. MgO, wt % (a) and Zr v. Nb, μg g^{-1} (b) showing the composition of Mahajanga mafic rocks. The data for Mahajanga rocks are from Melluso et al. (1997, 2002, 2003 and unpub. data).

3. Geochemical characteristics of the Mahajanga lavas

Representative major and trace element analyses of rocks of the northern part of the Madagascar Cretaceous igneous province are given in Table S1 in the online Supplementary Material (available at http://www.journals.cambridge.org/geo). The samples we have studied have previously been analysed for major elements, trace elements and Sr–Nd isotopes by Melluso et al. (1997, 2002, 2003). Melluso et al. (1997) identified two groups of rocks (A and C) in the Antanimena plateau. Both groups are tholeiitic and range from picritic basalt to basaltic andesite (MgO ranges from 13.2 to 3.3 wt %). The basalts and basaltic andesites are nearly aphyric and contain plagioclase, augite, pigeonite, Fe-Ti oxide and glass. Plagioclase and augite are the dominant phases, both as microphenocrysts and microlites in the groundmass. The picritic basalt (M422) has olivine phenocrysts set in an ophitic matrix of olivine, plagioclase, clinopyroxene and opaque oxides. Full details on the petrography and mineral compositions of these rocks can be found in Melluso, Morra & Fedele (2006) and Melluso et al. (1997).

Group A is a low Nb-Ti magma type (represented by samples M78, M83, M420 and M422) characterized by < 1.5 wt % TiO_2, 2–6 $\mu g\,g^{-1}$ Nb and 82–126 $\mu g\,g^{-1}$ Zr (Fig. 2). All Group A samples are mildly enriched in the light lanthanides (light rare earth elements (LREEs)), with La_n/Yb_n ranging from 1.4 to 4.1 (the subscript 'n' means chondrite normalized; Boynton, 1984). Their REE patterns are relatively flat in the middle and heavy REE portions of the pattern (Fig. 3a), with $Sm_n/Lu_n \approx 1.8$. Mantle-normalized incompatible element patterns of Group A lavas (Fig. 3b) display peaks at Ba and Pb and troughs at Th and Nb.

Group C consists of low Nb, high Ti-Fe lavas (e.g. M54, M87, M421 and Cava) with 2.1–2.6 wt % TiO_2, 14.4–15.6 wt % Fe_2O_{3t}, 121–200 $\mu g\,g^{-1}$ Zr and 3–9 $\mu g\,g^{-1}$ Nb (Fig. 2). Chondrite-normalized REE patterns for Group C rocks are comparable to those of Group A ($La_n/Yb_n = 3.0–4.5$; $La_n = 38–65$ times chondrite; Fig. 3a). In mantle-normalized multi-element patterns (Fig. 3b), the Group C rocks show a trough at Nb and peaks at Ba and Pb similar to those of Group A.

Igneous samples from the Bongolava–Manasamody plateau were also subdivided by Melluso et al. (1997) into two groups (B and D). They belong to tholeiitic series (from basalt to basaltic andesite) and are mostly aphyric, with rare plagioclase and augite microphenocrysts in a matrix of plagioclase, augite, orthopyroxene and/or pigeonite, Fe-Ti oxides and fresh glass. Microlites of olivine are present in a few samples of Group B and in the Tampoketsa Kamoreen basalts.

Group B (e.g. M32 and M60) is the most abundant magma type of the Mahajanga basin and shows moderate TiO_2 (2.2–2.5 wt %) and Nb (8–13 $\mu g\,g^{-1}$) and low K_2O and Rb (< 0.34 wt % and < 7 $\mu g\,g^{-1}$, respectively) contents (Fig. 2), and relatively high abundances of the LREEs ($La_n = 35–37$ times chondrite; Fig. 3c). In Figure 3d, the Group B basalts have peaks at Ba and troughs at K, and smoothly decreasing normalized abundances from La to Lu.

Group D basalts (e.g. M7a, M41, M45 and TK405; the Tampoketsa Kamoreen basalts belong to Group D) are characterized by high TiO_2 (3.3–4.9 wt %), Nb (15–24 $\mu g\,g^{-1}$) and Zr (217–327 $\mu g\,g^{-1}$) contents (Fig. 2). They are the most LREE enriched of the four magma groups, with La_n/Yb_n values of 5.6–7.8 and La_n contents of 64–98 times chondrite (Fig. 3c). They also have relatively smooth incompatible-element enriched patterns similar to those of present-day Marion hotspot basalts, except for Nb (Fig. 3d).

Alteration effects on major and trace elements appear minor. Most of the rocks studied are relatively fresh, as shown by low loss on ignition (LOI) values (Table S1 in the online Supplementary Material at http://www.journals.cambridge.org/geo) and by poor correlations between LOI and trace element contents.

The Antanimena rocks cover a wide range of $(^{87}Sr/^{86}Sr)_i$ and $(^{143}Nd/^{144}Nd)_i$ (corrected to 90 Ma), from 0.70331 to 0.70837 and from 0.51197 to 0.51253 ($\varepsilon Nd_i = +0.1$ to -10.8), respectively. The picritic basalt (M422) has the highest εNd_i and lowest $(^{87}Sr/^{86}Sr)_i$. The Bongolava–Manasamody rocks have less radiogenic $(^{87}Sr/^{86}Sr)_i$ (0.70377–0.70533) and more radiogenic εNd_i ($+1.0$ to $+4.0$) than the Antanimena rocks. Melluso et al. (2001, 2003) showed that there is a marked similarity between the geochemical features of the Antanimena rocks and those of the Mailaka district (tholeiitic series). Both have low Nb, Zr and εNd_i and high Ba and $(^{87}Sr/^{86}Sr)_i$ values (Fig. 4). The Bongolava–Manasamody rocks have trace element contents and Sr–Nd isotopic composition similar to lava flows of the Sambava sector and the Tamatave–Sainte Marie dyke swarm (Melluso et al. 2002; Fig. 4).

4. Review of published Madagascar Cretaceous Igneous Province ages: optimized age selection

Few ^{40}Ar–^{39}Ar ages are available for the Madagascar Cretaceous igneous province (Storey et al. 1995; Torsvik et al. 1998; Melluso et al. 2005). We have reviewed and filtered the published dataset based
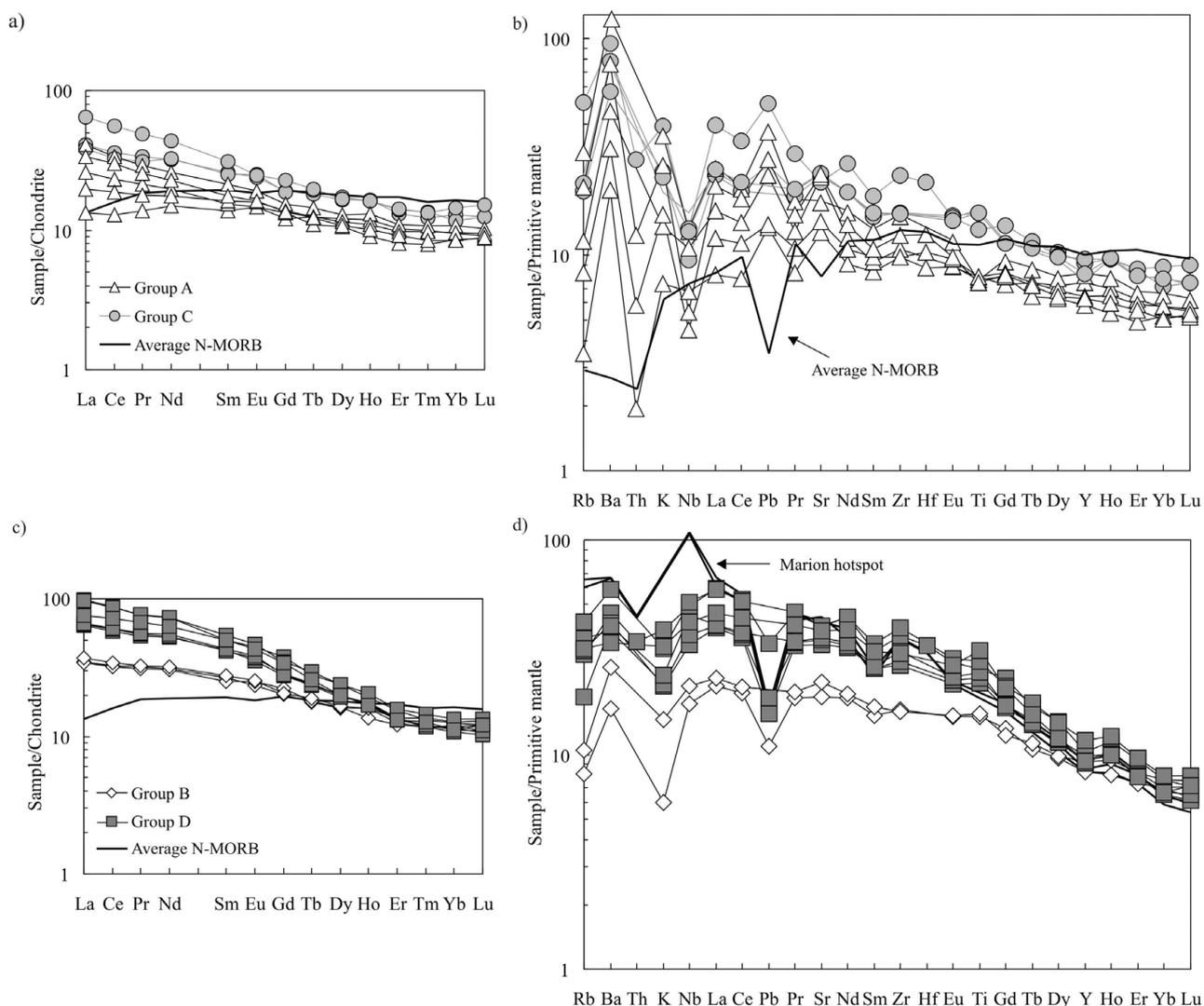
Figure 3. (a, c) Chondrite-normalized REE diagrams for Groups A and C and Groups B and D of the Mahajanga basin. Normalizing chondrite values are after Boynton (1984). (b, d) Primitive mantle-normalized incompatible element diagrams for Groups A and C and Groups B and D of the Mahajanga basin. Primitive mantle values are from Lyubetskaya & Korenaga (2007). Average normal mid-ocean ridge basalt (N-MORB) is from Niu & O'Hara (2003). Marion hotspot data are from Mahoney *et al*. (1992).

on the χ^2 statistical test approach (see Baksi, 2007*a,b*; Nomade *et al*. 2007; Jourdan *et al*. 2007) in order to screen out unreliable ages (Table S2 in the online Supplementary Material at http://www. journals.cambridge.org/geo). Even if harsh, we chose this approach as it allows unambiguous and secure assessment of ages of the different parts of the province and the duration of the province overall. In addition, the filtered ^{40}Ar–^{39}Ar ages have been recalculated using the new decay constants determined by Renne *et al*. (2010) so that these ages are fully comparable with U–Pb ages (see below). All the uncertainties associated with these ages (including systematic error on the decay constants) have been included (Table S3 in the online Supplementary Material at http://www.journals.cambridge.org/geo). We did not use published K–Ar ages for the Madagascar Cretaceous igneous province because of the high probability of post-eruptive alteration and/or excess ^{40}Ar and the impossibility of verifying either quantitatively, due

to the limitations of this technique (McDougall & Harrison, 1999).

Storey *et al*. (1995) reported 17 ^{40}Ar–^{39}Ar age determinations (made using whole-rock step heating and laser fusion of single and multiple feldspar grains) for basalt and rhyolite samples from the eastern coast of Madagascar (Sambava, Tamatave and Mananjary sectors), the Mahajanga (Bongolava plateau) and Morondava basins, and southern Madagascar (Volcan de l'Androy complex and Ejeda–Bekily dyke swarm). The ages range from 90 to 84 Ma, generally decreasing from north to south. While undoubtedly close to the crystallization age at the few million-year timescale, ^{40}Ar–^{39}Ar measurements performed on whole rocks are generally not trustworthy for old rocks, as they invariably contain cryptic alteration that can offset the age by as much as a few million years, even if a plateau is developed (e.g. Deccan Traps – Hofmann, Féraud & Courtillot, 2000; Central Atlantic Magmatic Province – Nomade *et al*. 2007; Karoo – Jourdan *et al*.
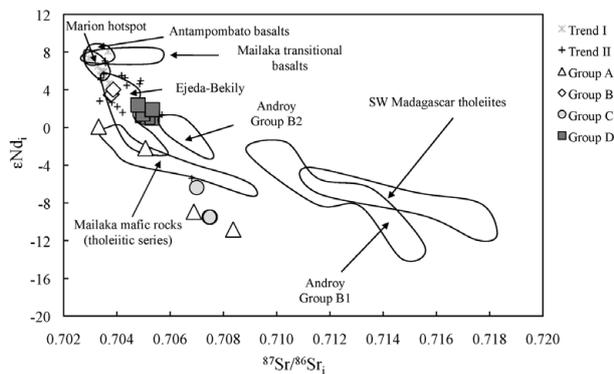
Figure 4. Sr and Nd isotopic compositions of Mahajanga rocks. The data for other basaltic rocks of the Madagascar igneous province are from Melluso *et al*. (2001, 2002, 2003, 2005), Storey, Mahoney & Saunders (1997), Mahoney, Nicollet & Dupuy (1991) and Mahoney *et al*. (2008). The high TiO_2 (> 3 wt %) basalts of Mananjary define Trend I. The Sambava and low TiO_2 (< 2 wt %) Mananjary basalts (including the high Mg-Ti basalts), and the Tamatave-Sainte Marie dyke swarm form Trend II.

2007). Furthermore, the laser fusion method applied to plagioclase is not a true step-heating approach. It is assumed that all grains would produce a 100 % plateau age and then an isochron is built from all the total fusion experiments. A 100 % plateau for plagioclase is demonstrated not to be the case for most of the Madagascar rocks (see below). Nevertheless, because of the relatively large uncertainty on these ages (typically ± 1 to ± 10 Ma), these results are likely to approach the true age within error.

Torsvik *et al*. (1998) reported an ^{40}Ar–^{39}Ar age of 83.6 ± 1.6 Ma (using whole-rock step heating) for a basalt from the southwestern part of the Morondava basin. Although the sample yielded a 'mini-plateau' with 56 % of the gas, the shape of the spectrum is seriously perturbed. Therefore, this age is not considered reliable for the purpose of high-precision geochronology.

None of the reported ^{40}Ar–^{39}Ar data from the Antampombato–Ambatovy intrusion (Melluso *et al*. 2005) meet the definition of a plateau and the shape of the spectra is highly structured, and the use of the isochron to calculate an age is not correct. If there is indeed excess Ar, then most if not all the points should fit on the isochron; otherwise, selecting the points at the bottom of the saddle shape will produce a spurious arbitrary result. These ages are undoubtedly close to the crystallization age ($\approx$ 89 Ma), but can have easily been shifted by 3–4 Ma either way.

Plagioclase separates from the rhyolite of the Sakanila massif (eastern Madagascar) yielded a reliable ^{40}Ar–^{39}Ar age of 88.7 ± 0.6 Ma (MSWD, mean standard weighted deviation = 1.75; Cucciniello *et al*. 2011).

Four zircon U–Pb ages are available for the Madagascar Cretaceous igneous province. Two are for the capping rhyodacitic unit of the Mailaka lava succession (89.7 ± 1.4 Ma and 90.7 ± 1.1 Ma; Cucciniello *et al*. 2010). The other two ages are for the Analalava gabbro

intrusion (weighted mean ^{206}Pb–^{238}U age of 91.6 ± 0.3 Ma for all analyses of zircon and baddeleyite; Torsvik *et al*. 1998) and Antampombato–Ambatovy complex (90.0 ± 2.0 Ma; Melluso *et al*. 2005). Zircons and baddeleyites from the sample of the Analalava intrusion do not yield concordant results and only one of the two populations can be used to calculate the age of the gabbro as they record different events. In general, zircon is the mineral of choice for U–Pb dating of silicic volcanic rocks as it usually provides the most reliable ages owing to its robustness to alteration, although we note that it can often yield an age offset of 0.1 and up to 0.6 Ma because of its residence time in a magma chamber (e.g. Simon, Renne & Mundil, 2008). Hereafter, we consider the zircon U–Pb age of 91.8 ± 0.2 Ma as the best estimate for the crystallization age of the Analalava gabbro.

5. ^{40}Ar–^{39}Ar results

Detailed ^{40}Ar–^{39}Ar results for the two samples from the Antanimena plateau (belonging to the A group) are shown in Tables 1 and 2. Plagioclase separated from picritic basalt M422 gave a plateau age of 92.3 ± 2.0 Ma (MSWD = 1.21 and probability, P, value of 0.29; 2σ, all uncertainty included; Fig. 5a) including 77.8 % of the ^{39}Ar released. The inverse isochron age (90.4 ± 3.3 Ma; MSWD = 1.06) is within two standard deviations of the plateau age (Fig. 5a) and the isochron has an initial $^{40}Ar/^{36}Ar$ ratio of 307 ± 16 within error of the value of the atmospheric ratio adopted in this study (295.5).

Plagioclase separated from tholeiitic basalt M420 yielded a well-defined plateau age of 91.5 ± 1.3 Ma (MSWD = 0.38; P = 0.96; Fig. 5b), defined by 98.7 % of the total ^{39}Ar released. The inverse isochron age (91.5 ± 1.3 Ma) and initial $^{40}Ar/^{36}Ar$ ratio (296 ± 8) are indistinguishable from the plateau age and air ratio, respectively.

The two plateau ages of 92.3 ± 2.0 and 91.5 ± 1.3 Ma determined for the Antanimena plateau are indistinguishable. In addition, these ages are in agreement within uncertainties, with the U–Pb ages of ∼ 90–92 Ma obtained for the Analalava intrusion and the capping rhyodacitic unit of the Mailaka lava succession (Torsvik *et al*. 1998; Cucciniello *et al*. 2010).

6. Age and duration of the northern part of the Madagascar Cretaceous igneous province

The new ages obtained in this study suggest that the magmatism in the western Mahajanga basin (Antanimena plateau) started about 92 Ma ago. These ages are close to although distinctly younger than the Cenomanian–Turonian (C–T; 93.6 ± 0.8 Ma; Gradstein, Ogg & Smith, 2005) boundary and are indistinguishable from the U–Pb ages available for this part of the province ranging from 89.7 ± 1.4 Ma and 90.7 ± 1.1 Ma (Cucciniello *et al*. 2010). The ^{40}Ar–^{39}Ar ages of 89.0 ± 5.9 and 87.6 ± 3.7 Ma reported

Table 1. Ar data summary for individual aliquots of Mahajanga plagioclase separates

Sample no.	Temperature (°C)	$^{36}Ar \pm \sigma$ (V)		$^{37}Ar \pm \sigma$ (V)		$^{38}Ar \pm \sigma$ (V)		$^{39}Ar \pm \sigma$ (V)		$^{40}Ar \pm \sigma$ (V)		$^{40}Ar^*$ (%)	$^{40}Ar^*/^{39}Ar_K \pm \sigma$		Age $\pm \sigma$ (Ma)	
M420	*D = 1.00129*			*J = 0.0068800 ± 0.0000234*												
9A6489D	500	0.018934	0.000044	0.000443	0.000020	0.003806	0.000063	0.005167	0.000048	5.598409	0.002388	1.0	10.81	± 16.45	129.43	± 190.09
9A6490D	550	0.003502	0.000053	0.001650	0.000036	0.003094	0.000038	0.188198	0.000274	2.198461	0.001567	63.7	7.45	± 0.15	90.19	± 1.81
9A6491D	620	0.001350	0.000021	0.002368	0.000028	0.003213	0.000064	0.264616	0.000194	2.048632	0.001469	97.9	7.60	± 0.11	92.00	± 1.28
9A6492D	700	0.001268	0.000024	0.002086	0.000030	0.003351	0.000043	0.261488	0.000489	2.019282	0.001376	97.0	7.50	± 0.10	90.74	± 1.18
9A6493D	780	0.000877	0.000017	0.001417	0.000036	0.002244	0.000032	0.172981	0.000152	1.350953	0.000733	96.3	7.60	± 0.13	91.93	± 1.54
9A6494D	860	0.000731	0.000025	0.001126	0.000041	0.001445	0.000027	0.109713	0.000194	0.876563	0.000751	94.1	7.41	± 0.14	89.72	± 1.69
9A6495D	940	0.000534	0.000011	0.000854	0.000029	0.001080	0.000020	0.076471	0.000133	0.617236	0.000290	94.0	7.39	± 0.14	89.41	± 1.65
9A6496D	1020	0.000443	0.000013	0.000745	0.000033	0.001248	0.000028	0.083029	0.000139	0.661635	0.000573	95.9	7.42	± 0.12	89.80	± 1.47
9A6497D	1100	0.000449	0.000008	0.000661	0.000019	0.000949	0.000019	0.048405	0.000072	0.425542	0.000443	89.5	7.49	± 0.17	90.64	± 1.98
9A6498D	1200	0.001428	0.000021	0.002346	0.000051	0.000687	0.000027	0.038307	0.000087	0.328108	0.000375	83.1	7.02	± 0.80	85.12	± 9.42
9A6499D	1300	0.000374	0.000014	0.000527	0.000025	0.000277	0.000010	0.015651	0.000077	0.178258	0.000281	79.4	7.17	± 0.55	86.88	± 6.46
9A6500D	1400	0.000424	0.000010	0.000569	0.000025	0.000218	0.000012	0.009710	0.000045	0.162631	0.000388	89.7	9.49	± 0.86	114.11	± 20.02
9A6501D	1550	0.000713	0.000012	0.000556	0.000021	0.000218	0.000017	0.007693	0.000042	0.223793	0.000811	91.7	10.34	± 1.09	123.97	± 25.18
M422	*D = 1.001286*			*J = 0.0070540 ± 0.0000148*												
9A6534D	550	0.024991	0.000100	0.000859	0.000045	0.005995	0.000132	0.032269	0.000126	7.329391	0.005161	1.1	2.56	± 3.49	32.34	± 43.58
9A6535D	600	0.001066	0.000010	0.000819	0.000033	0.001421	0.000037	0.101755	0.000246	0.909692	0.000679	77.6	6.88	± 0.14	85.48	± 1.65
9A6536D	650	0.002910	0.000033	0.001110	0.000040	0.002400	0.000025	0.150696	0.000256	1.774922	0.001399	61.1	7.18	± 0.15	89.13	± 1.78
9A6537D	700	0.003747	0.000038	0.001100	0.000032	0.002017	0.000031	0.106949	0.000350	1.729667	0.002564	45.8	7.42	± 0.23	91.98	± 2.77
9A6538D	750	0.002223	0.000015	0.001082	0.000030	0.001323	0.000030	0.076682	0.000122	1.049323	0.000675	53.5	7.30	± 0.23	90.59	± 2.80
9A6539D	800	0.001679	0.000022	0.000992	0.000043	0.000956	0.000016	0.052434	0.000147	0.756821	0.000557	54.8	7.85	± 0.34	97.26	± 4.05
9A6540D	900	0.002372	0.000025	0.000922	0.000021	0.001148	0.000020	0.057962	0.000171	1.018061	0.000632	44.9	7.84	± 0.30	97.09	± 3.67
9A6541D	1000	0.002128	0.000019	0.001439	0.000026	0.002202	0.000038	0.146226	0.000211	1.500126	0.001035	73.6	7.52	± 0.14	93.20	± 1.75
9A6542D	1100	0.001782	0.000020	0.001936	0.000041	0.002270	0.000021	0.155184	0.000205	1.333225	0.000912	84.4	7.23	± 0.17	89.71	± 2.09
9A6544D	1200	0.002599	0.000027	0.003721	0.000023	0.003211	0.000035	0.236330	0.000473	1.819422	0.000334	93.1	7.21	± 0.21	89.47	± 2.60
9A6545D	1300	0.001010	0.000019	0.001437	0.000029	0.001037	0.000023	0.074649	0.000205	0.578398	0.000383	90.3	6.66	± 0.32	82.86	± 3.85
9A6546D	1400	0.001342	0.000016	0.001656	0.000016	0.000928	0.000029	0.066310	0.000079	0.545028	0.000790	82.4	6.17	± 0.38	76.82	± 4.69
9A6547D	1500	0.000641	0.000015	0.000581	0.000022	0.000212	0.000007	0.006738	0.000047	0.165648	0.000431	57.7	6.02	± 1.83	75.07	± 22.28

Values are corrected for mass discrimination, blanks and radioactive decay. Uncertainties are given at the 1σ level. $^{40}Ar^*$ – radiogenic argon. J – irradiation parameter. Age is based on comparison with the GA1550.

Table 2. Summary table indicating plateau and isochron ages for the Mahajanga plagioclase separates

Sample	Material	Integrated age (Ma ± 2σ)	Plateau age (Ma ± 2σ)	MSWD	P	Total ^{39}Ar released (%)	Isochron age (Ma ± 2σ)	^{40}Ar/^{36}Ar intercept (± 1σ)	MSWD isochron
M422	plagioclase	88 ± 2.7	92.3 ± 2.0	1.21	0.29	77.8	90.4 ± 3.3	306.6 ± 16.2	1.06
M420	plagioclase	91.2 ± 2.1	91.5 ± 1.3	0.38	0.96	98.7	91.5 ± 1.3	295.8 ± 8.3	0.42

MSWD for plateau and inverse isochron, probability (P) for plateau, percentage of ^{39}Ar degassed used in the plateau calculation and ^{40}Ar/^{36}Ar intercept are indicated. Analytical uncertainties on the ages are quoted at 2 sigma (2σ).

by Storey *et al.* (1995; recalculated using the new decay constants determined by Renne *et al.* 2010) for the Bongolava–Manasamody plateau overlap or are marginally younger within uncertainty than the ages obtained in this study. The large uncertainty of these apparent ages, however, precludes their use to estimate the duration of the emplacement of the lava pile. In addition, as discussed in Section 4, the validity of the ages obtained using the whole-rock step-heating method and laser fusion of single and multiple feldspar grains can be compromised and are deemed unreliable for high-precision geochronology, because of potential cryptic alteration, recoil and/or excess argon problems. Two new ^{40}Ar–^{39}Ar and four previously published U–Pb ages are altogether statistically distinguishable (P = 0.007) and therefore, can be used to estimate the duration of the magmatic activity of this part of the Madagascar Cretaceous igneous province. A standard deviation of ± 1.0 Ma and a mid-peak width of 2 Ma on the probability density distribution plot (not shown; n = 6), suggest an approximated duration on the order of ∼ 2 Ma. Note, however, that this does not preclude

that the bulk of the magmatic volume erupted in a shorter time span although volcanic intrusions occurred over a slightly longer period. Nevertheless, the age of emplacement of the Mahajanga flood basalt sequence can be fully addressed using a larger dataset.

7. Isotope geochemistry

Lead isotope compositions for the Mahajanga rocks are presented in Table 3 and in Figure 6a and b. The Antanimena rocks (Groups A and C) have very low ^{206}Pb/^{204}Pb (15.283–16.325), ^{207}Pb/^{204}Pb (15.058–15.269) and ^{208}Pb/^{204}Pb (35.483–36.547). Their Pb isotope ratios correlate well with each other (Fig. 6a, b). The Bongolava–Manasamody basalts (Groups B and D) have higher ^{206}Pb/^{204}Pb (16.518–17.355) and ^{208}Pb/^{204}Pb (37.511–38.009) than the Antanimena samples, but similar ^{207}Pb/^{204}Pb (15.086–15.404). As shown in Figure 6a, the Antanimena and Bongolava–Manasamody data define separate arrays to the left of the 4.55 Ga geochron towards low-^{206}Pb/^{204}Pb compositions. In the ^{208}Pb/^{204}Pb v. ^{206}Pb/^{204}Pb diagram
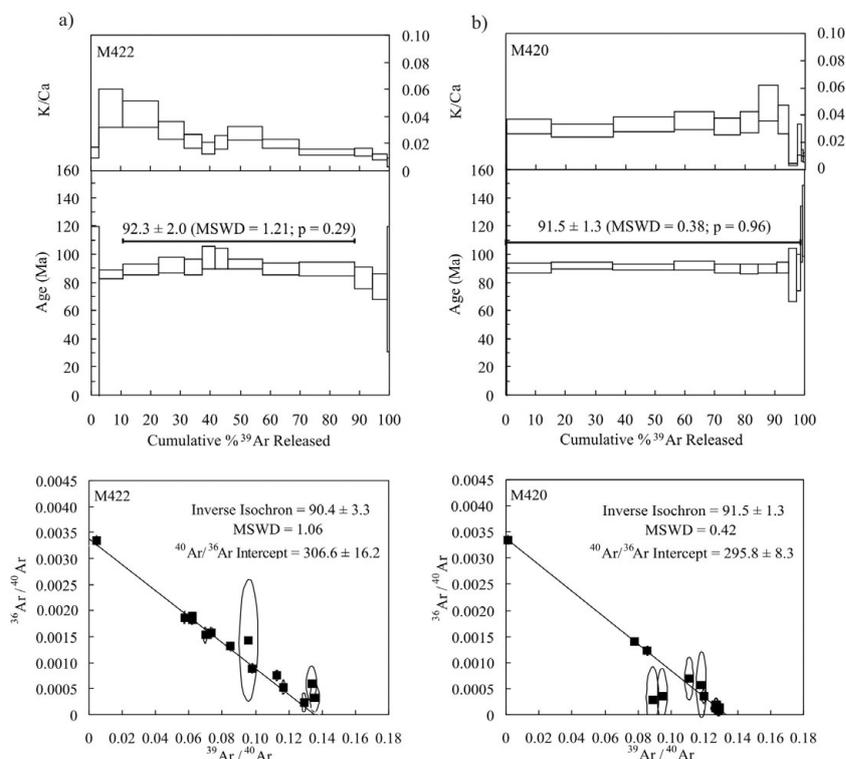
Figure 5. Plagioclase age spectra and inverse isochron plots for basaltic rocks from the Antanimena plateau. The horizontal lines close to the plateau age indicate the steps used in the age calculation. Errors on plateau ages (plateaus include > 70 % ^{39}Ar released) are quoted at 2σ and include all sources of uncertainties. MSWD, P values and ^{40}Ar/^{36}Ar intercept are indicated.

Table 3. Sr, Nd and Pb isotopic data for volcanic rocks from Mahajanga basin

Sample	Type	Group	$^{87}Sr/^{86}Sr$	$(^{87}Sr/^{86}Sr)_i$	$^{143}Nd/^{144}Nd$	$(^{143}Nd/^{144}Nd)_i$	εNd_i	Pb, $\mu g\,g^{-1}$	$^{206}Pb/^{204}Pb$	$^{207}Pb/^{204}Pb$	$^{208}Pb/^{204}Pb$
M422	picr bas	A	0.70334	0.70331	0.512635	0.512528	0.1		15.871	15.126	35.857
M420	tho bas	A	0.70513	0.70507	0.512517	0.512412	−2.2	1.98	16.325	15.269	36.547
M78	bas and	A	0.70707	0.70689	0.512160	0.512066	−8.9	5.29	15.283	15.061	35.684
M83	bas and	A	0.70842	0.70837	0.512060	0.511970	−10.8				
M2	tho bas	B	0.70391	0.70386	0.512830	0.512730	4.0				
M32	tho bas	B	0.70384	0.70379	0.512800	0.512704	3.5	1.58	17.355	15.404	37.899
M60	tho bas	B	0.70379	0.70377	0.512800	0.512701	3.4	1.44	17.327	15.404	37.880
M54	bas and	C	0.70760	0.70750	0.512130	0.512037	−9.5				
M87	bas and	C	0.70757	0.70746	0.512130	0.512037	−9.5	3.72	15.320	15.058	35.483
M421	bas and	C	0.70725	0.70700	0.512279	0.512197					
M7a	tho bas	D	0.70541	0.70533	0.512700	0.512620	1.9	4.73	16.671	15.123	38.009
M26	tho bas	D	0.70521	0.70515	0.512670	0.512580	1.1				
M33	tho bas	D	0.70543	0.70532	0.512660	0.512574	1.0				
M41	tho bas	D	0.70508	0.70498	0.512690	0.512597	1.4	2.23	17.075	15.279	37.511
M45	tho bas	D	0.70507	0.70496	0.512680	0.512590	1.3	2.66	16.518	15.086	37.901
TK405	tho bas	D	0.70488	0.70479	0.512737	0.512646	2.4				

Sr and Nd isotopic ratios are from Melluso *et al*. (1997, 2002, 2003). Measured isotope ratios are age-corrected (subscript i) to 90 Ma. Pb isotope ratios are reported relative to the NBS 981 Pb values of Todt *et al*. (1996). Reproducibility for NBS was ± 0.011 for $^{206}Pb/^{204}Pb$ and $^{207}Pb/^{204}Pb$, and ± 0.031 for $^{208}Pb/^{204}Pb$. Within-run 2σ errors on the tabulated data were less than or equal to ± 0.008 for $^{206}Pb/^{204}Pb$, ± 0.011 for $^{207}Pb/^{204}Pb$ and ± 0.032 for $^{208}Pb/^{204}Pb$. Total procedural blanks were negligible at < 19 pg for Pb. The relative uncertainty for Pb concentrations measured by isotope dilution is 0.5 %. Measurements were made at the University of Hawaii. picr bas – picritic basalt; tho bas – tholeiitic basalt; bas and – basaltic andesite.

(Fig. 6b), the Antanimena data form an array displaced towards higher $^{208}Pb/^{204}Pb$ than the Northern Hemisphere Reference Line (NHRL; Hart, 1984), whereas the Bongolava–Manasamody data display a slightly negative slope towards higher $^{208}Pb/^{204}Pb$. Pb isotope differences between the Antanimena and Bongolava–Manasamody rocks reflect the geochemical characteristics of the magma sources and contaminants.

The basaltic rocks of the Madagascar province cover a wide range in Pb isotope compositions (Fig. 6a, b). However, only a few samples (from the eastern coast; Trend II) show low Pb isotope values similar to Mahajanga rocks (Fig. 6a, b). The low $^{206}Pb/^{204}Pb$ and $^{207}Pb/^{204}Pb$ compositions suggest that Mahajanga magmas interacted with old, U-depleted continental crust. In contrast, the fields defined by tholeiitic rocks from the southern part of the Madagascar province are consistent with assimilation of crustal material with high $^{206}Pb/^{204}Pb$, $^{207}Pb/^{204}Pb$ and $^{208}Pb/^{204}Pb$ ratios.

Re–Os isotopic data for the four magma groups from the Mahajanga area are reported in Table 4. With the exception of the picritic basalt M422 (Group A), with an Os content of 0.8 ng g^{-1}, all of the basaltic rocks of the four magma groups have very low Os contents, from 0.004 to 0.032 ng g^{-1} (Table 4). The Re contents and hence Re/Os ratios of the basaltic rocks are highly variable. Two samples (Cava and TK405) have higher Re contents (Re = 0.108–0.144 ng g^{-1}) than the other basaltic rocks with similar MgO (Re = 0.038–0.048 ng g^{-1}). The lowest Re content was found in the picritic basalt (Re = 0.009 ng g^{-1}). The $^{187}Re/^{188}Os$ ratios vary widely within the basaltic rocks, ranging from 0.0573 to 445. Initial Os isotopic ratios of the four magma groups span a large range, with $(^{187}Os/^{188}Os)_i$ varying from 0.1408 to 9.4524 (γ_{Os} = +11 to +7378; γ_{Os} values are calculated at 90 Ma, assuming a chondritic mantle $^{187}Os/^{188}Os$ ratio of 0.127, Walker & Morgan, 1989; Table 4). In the εNd_i v. $(^{187}Os/^{188}Os)_i$ diagram (Fig. 6c),

Table 4. Re–Os isotopic data for volcanic rocks from Mahajanga basin

Sample	M422	M32	Cava	M7a	TK405
Type	picr bas	tho bas	bas and	tho bas	tho bas
Group	A	B	C	D	D
Re	0.009	0.038	0.144	0.048	0.108
Os	0.800	0.032	0.004	0.011	0.009
Re/Os	0.01	1.19	40.08	4.36	12.14
$^{187}Re/^{188}Os$	0.1	5.9	444.9	22.7	70.7
$^{187}Os/^{188}Os$	0.1409	0.2968	10.1200	0.7390	1.7270
$(^{187}Os/^{188}Os)_i$	0.1408	0.2880	9.4524	0.7049	1.6209
γ_{Os}	11	128	7378	458	1182

Abundances for Re and Os are in ng g^{-1}.
$\gamma_{Os} = [(^{187}Os/^{188}Os_{sample}/^{187}Os/^{188}Os_{mantle}) − 1] \times 100$ using an estimated average chondritic mantle $^{187}Os/^{188}Os = 0.127$ (Walker & Morgan, 1989).

data for the Mahajanga rocks show a trend that indicates the involvement of a contaminant with high Os isotopic ratios, such as the continental crust (e.g. γ_{Os} = + 330 to +22 000; McBride *et al*. 2001 and references therein). The Mahajanga rocks (Groups B and D) show distinctly more radiogenic $(^{187}Os/^{188}Os)_i$ than the Mailaka rocks (Fig. 6c).

8. Crustal contamination

No closed system model can explain the wide trace element and isotopic variations observed in the Mahajanga rocks. The Antanimena rocks (Groups A and C) have high Ba/Nb (33–156), Sr/Nd (13–31) and low Ce/Pb (5–8) and Nb/La (0.3–0.8), similar to crustal materials (Fig. 7a). In contrast, the Bongolava–Manasamody basalts (Groups B and D) have lower Ba/Nb (9–14), Sr/Nd (14–18) and higher Ce/Pb (15–21) and Nb/La (0.8–1.0; Fig. 7a). In the εNd_i v. SiO$_2$ diagram (Fig. 7b), the Antanimena rocks display a general negative correlation, possibly indicating the influence of crustal materials. Although Group D
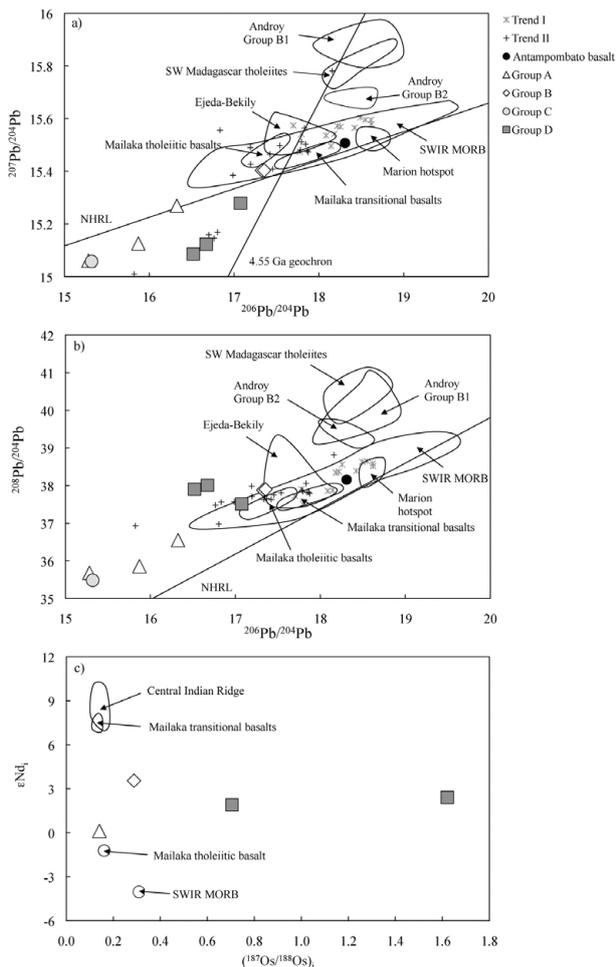
Figure 6. (a–c) Pb and Os isotopic compositions of Mahajanga rocks. In Pb–Pb isotope space (a–b), the Northern Hemisphere Reference Line (NHRL) and the Geochron at 4.55 Ga are also shown. The data for other basaltic rocks of the Madagascar igneous province are from Melluso *et al.* (2001, 2002, 2003, 2005 and unpub. data), Cucciniello *et al.* (2010), Storey, Mahoney & Saunders (1997), Mahoney, Nicollet & Dupuy (1991) and Mahoney *et al.* (2008). Fields for modern Marion hotspot and Southwest Indian Ridge (SWIR) MORB data are from are from Mahoney *et al.* (1992), Janney, le Roex & Carlson (2005) and Meyzen *et al.* (2005). (c) Fields for Mailaka transitional and tholeiitic basalts are from Cucciniello *et al.* (2010). Central and Southwest Indian Ridge data are from Escrig *et al.* (2004).

basalts exhibit a slightly negative correlation in the εNd_i v. SiO_2 diagram (Fig. 7b), the small range of their isotopic values could preclude a substantial involvement of crustal rocks in their genesis. The small range could also indicate that the magmas were generated in large crustally contaminated magma chambers that were homogenized. The high εNd_i values indicate that contamination was not too significant.

Pb isotopic values of Group A, C and D basalts overlap the fields defined by worldwide xenoliths from lower cratonic crust and Archaean crust (Fig. 8), suggesting that the crustal contaminant was old U-depleted continental crust. We suggest that the Archaean rocks of northern Madagascar are plausible contaminants for the Mahajanga magmas. The basement rocks exposed in
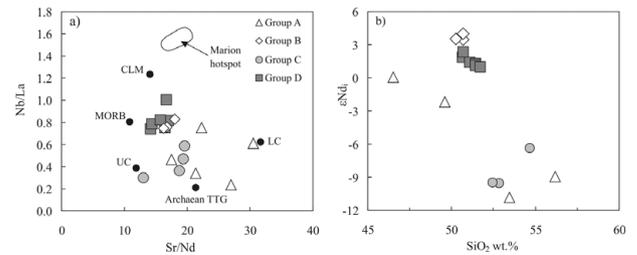
Figure 7. (a) Nb/La v. Sr/Nd diagram, showing the composition of Mahajanga lavas; UC – average upper continental crust (Rudnick & Gao, 2003); LC – average lower continental crust (Rudnick & Gao, 2003); Archaean crust (Condie, 2005); Average N-MORB (Niu & O'Hara, 2003); CLM – average continental lithospheric mantle from peridotite xenoliths (Simon *et al.* 2007); Marion hotspot field (Janney, le Roex & Carlson, 2005). (b) εNd_i v. SiO_2 diagram for the Mahajanga lava compositions.
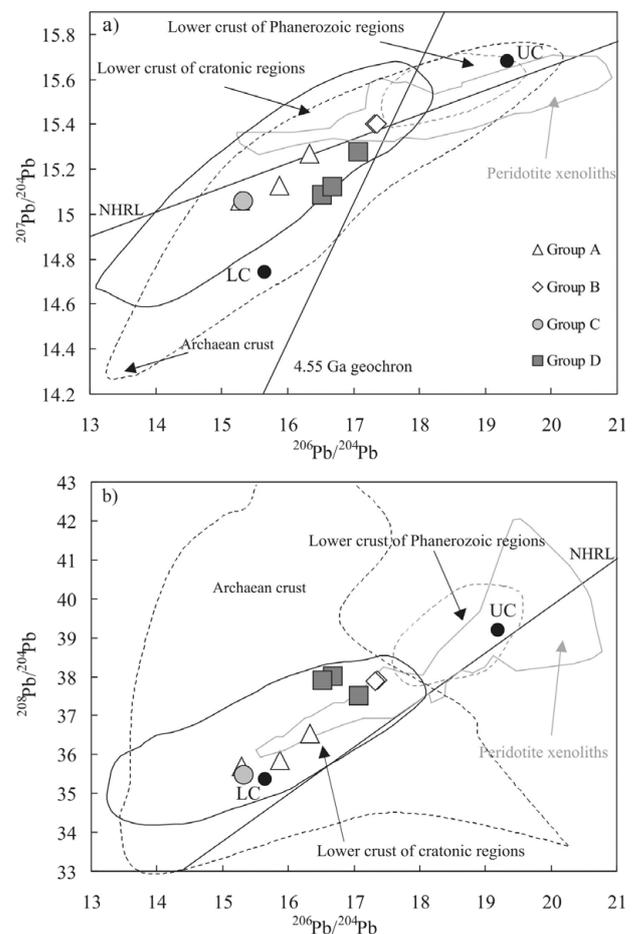
Figure 8. (a, b) $^{208}Pb/^{204}Pb$ and $^{207}Pb/^{204}Pb$ v. $^{206}Pb/^{204}Pb$ for Mahajanga rocks. Fields for lower crustal xenoliths (beneath cratonic and Phanerozoic regions), peridotite xenoliths and Archaean crust are from Downes *et al.* (2001), Meyzen *et al.* (2005), Kreissig *et al.* (2000) and Sengupta *et al.* (1991). UC – total upper crust (Kramers & Tolstikhin, 1997); LC – total lower crust (Kramers & Tolstikhin, 1997).

northern Madagascar are dominated by orthogneisses and paragneisses that were metamorphosed and partially melted under granulite- and upper amphibolite-facies conditions in Neoarchaean time (De Waele *et al.* 2011 and reference therein). High-grade metamorphism and crustal melting could have produced the low-μ
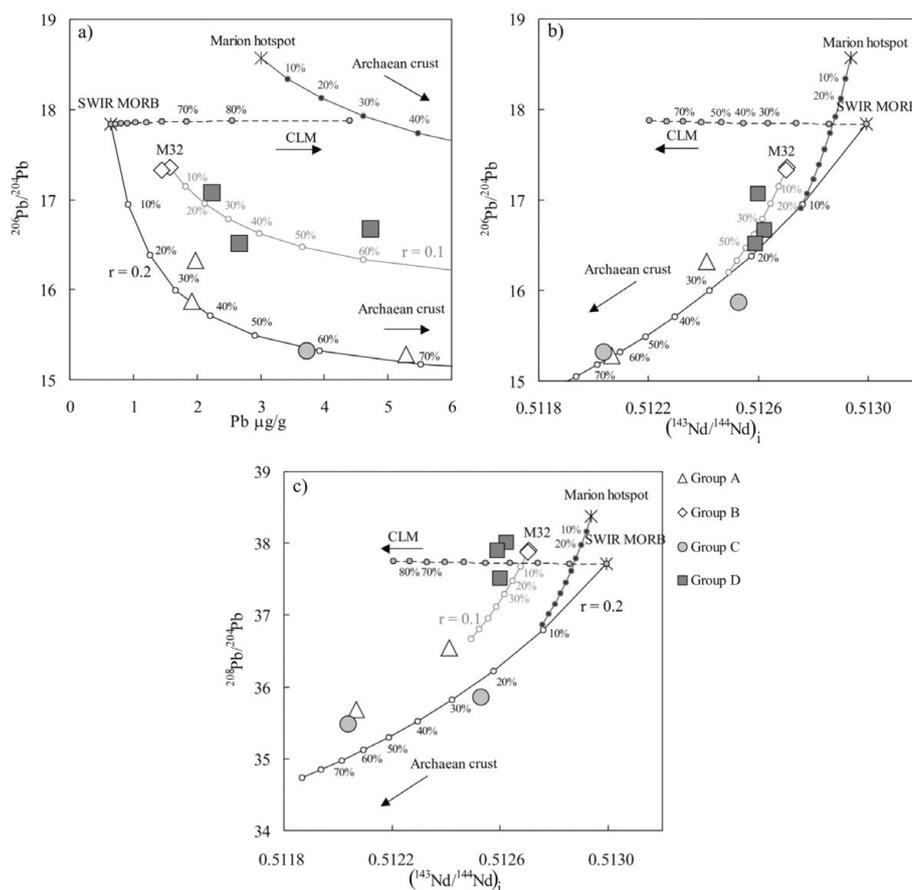
Figure 9. (a–c) $^{206}Pb/^{204}Pb$ v. Pb ($\mu g\ g^{-1}$), and $^{206}Pb/^{204}Pb$ and $^{208}Pb/^{204}Pb$ v. $(^{143}Nd/^{144}Nd)_i$ for Mahajanga rocks. Four AFC models are illustrated. The AFC calculations were run for the Antanimena (black curves) and Bongolava–Manasamody (Group D) rocks (grey curves), using two different mantle-derived basalt and crustal end-members. Numbers on the AFC curves indicate the residual liquid fraction. Assumed bulk partition coefficients: $D_{Nd} = 0.2$, $D_{Pb} = 0.2$. $r = mass_{assimilated}/mass_{accumulated}$. Crustal contaminant values used in the AFC modelling are from Möller, Mezger & Schenk (1998; sample A159–1) and Kreissig *et al*. (2000; sample 96/217). Continental lithospheric contaminant values are from Walker *et al*. (1989; sample 1008-Cpx). Starting composition for the Antanimena rocks is a SWIR MORB (AII 93–5/1; Mahoney *et al*. 1989). AFC modelling with Marion hotspot values for the starting material (dark grey curves) is also reported.

($\mu = ^{238}U/^{204}Pb$) signature. In addition, the different trends in Figure 6a and b indicate the involvement of crustal assimilants with different time-integrated U/Pb and Th/Pb ratios. Cucciniello *et al*. (2010) already reported evidence of contamination by variable upper-to-lower crustal contaminants in the evolved rocks of the Mailaka sequence, which suggests that these processes are not uncommon in the Madagascar Cretaceous igneous province.

The Group B basalts most likely experienced minimal crustal contamination (on the basis of trace element and Sr–Nd–Pb isotopic ratios), and we believe that their isotopic compositions may reflect the isotopic features of their mantle source. In Figure 8, the isotopic data for the Group B basalts fall in the field defined by worldwide peridotite xenoliths.

To better evaluate the crustal components in the Mahajanga magmas, we used the fractional crystallization (AFC) model of DePaolo (1981). The AFC modelling using the Os isotopic data does not provide any further information about the nature of the crustal contaminant given the very low Os contents of the samples (Table 4). If the contaminant has relatively high Os contents (e.g.

0.05 ng g^{-1}) and high $^{187}Os/^{188}Os$ (e.g. > 1), very low degrees of crustal contamination can produce a radiogenic $^{187}Os/^{188}Os$ signature in the magmas.

The compositions of the contaminants chosen for the modelling are those of Archaean crustal rocks of South Africa (Kreissig *et al*. 2000) and Tanzania (Möller, Mezger & Schenk, 1998), because no whole-rock Pb isotopic data have been published for Madagascan continental crust to date. In the AFC modelling, the mantle-derived parental magmas chosen for the Antanimena and Bongolava–Manasamody rocks are a Southwest Indian Ridge (SWIR) MORB (Mahoney *et al*. 1989) and Bongolava basalt (M32; this study), respectively. The results show that the sample M41 (Group D) and the picritic basalt (M422) of Antanimena are the least contaminated. A maximum assimilated mass of ~ 14 % is required to produce the evolved rocks of Antanimena (Fig. 9). In addition, the AFC calculations indicate the involvement of a crustal contaminant with variable $^{208}Pb/^{204}Pb$ ratios in the genesis of the Group D basalt.

The very low $^{206}Pb/^{204}Pb$ and $^{207}Pb/^{204}Pb$ signatures observed in the Mahajanga rocks (Fig. 8) rule out the involvement of lithospheric mantle as a contaminant
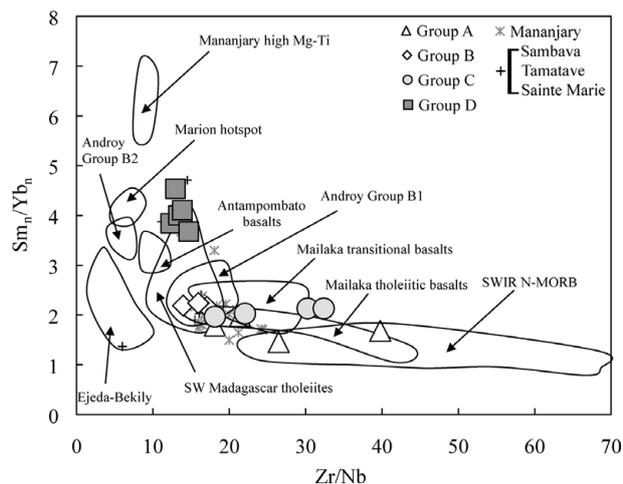
Figure 10. Sm_n/Yb_n v. Zr/Nb for Mahajanga rocks. The data for other basaltic rocks of the Madagascar igneous province are from Melluso *et al.* (2001, 2002, 2003, 2005), Cucciniello *et al.* (2011), Storey, Mahoney & Saunders (1997), Dostal *et al.* (1991) and Mahoney *et al.* (2008). Fields for modern Marion hotspot and (SWIR) N-MORB are from Mahoney *et al.* (1992) and Janney, le Roex & Carlson (2005).

in their genesis. The results of AFC modelling support this interpretation.

9. Mantle sources

Most of the Mahajanga rocks have experienced extensive fractional crystallization and crustal contamination (Melluso *et al.* 1997, 2003), but the regional trace element heterogeneity of the Mahajanga flood basalt sequence cannot be explained only by these two processes. In order to evaluate the mantle source characteristics, we prefer to use element ratios involving HFSEs and HREEs, such as Zr/Y, Sm/Yb and Zr/Nb, which are not strongly modified by fractional crystallization or crustal contamination processes.

The Mg-rich Group A basalts (M422, M420) have low Zr/Y (3.3–3.8), Sm_n/Yb_n (1.5–1.7) and high Zr/Nb (> 20) ratios typical of normal MORB, whereas Group B and D basalts have high Zr/Y (4.3–8.7), Sm_n/Yb_n (2.2–4.5) and low Zr/Nb (< 18) typical of magmas derived from incompatible- element-enriched mantle (Fig. 10). In addition, the high Sm_n/Yb_n and Zr/Y ratios indicate the presence of residual garnet in the source of the Group D basalts, whereas the low Sm_n/Yb_n and Zr/Y ratios observed in the other groups exclude melting in the presence of residual garnet (cf. Melluso *et al.* 2002, 2003, 2005).

The role of the Marion hotspot as a heat or melt source in the genesis of the Madagascar basalts is controversial (Storey, Mahoney & Saunders, 1997; Melluso *et al.* 1997, 2002, 2003; Mahoney *et al.* 2008). The Mailaka and Antampombato transitional basalts have Sr and Nd isotope ratios similar to those of present-day Marion hotspot basalts, but their Pb isotopic and trace element compositions are different (Fig. 6). The geochemical imprint of the Marion hotspot seems evident in some Fe-Ti basalts (Trend I;

Storey, Mahoney & Saunders, 1997) of Mananjary, whereas in the Androy complex (close to the postulated position of the Marion hotspot at 88 Ma) a Marion-like isotopic signature is absent (Mahoney *et al.* 2008). The Antanimena basalts do not resemble hotspot-derived magmas. Although, the picritic basalt (M422) shows Sr–Nd–Os isotopic characteristics similar to ocean island basalt (OIB; e.g. McBride *et al.* 2001 and reference therein), its Pb isotope values are lower and equivalent to those of the continental crust (Fig. 8). In contrast, the Group D basalts have incompatible element patterns resembling those of present-day Marion hotspot basalts (Fig. 3d). However, because of crustal contamination, the isotopic compositions of Group D basalts cannot provide much information about the composition of the mantle source. Only the isotopic compositions of the least contaminated Group B basalts could approach that of the mantle source. The Group B basalts have compositions that can be readily attributed to lithospheric materials (Fig. 6). Figure 9 shows that AFC modelling (assuming present-day Marion hotspot lavas are representative of the parental magma of the Group B and D basalts) cannot reproduce the isotopic variations of either magma type. Numerical modelling of the Mahajanga basalts (cf. Melluso *et al.* 2002, 2003, 2005) indicates mixing relationships between partial melts of MORB-like mantle and partial melts of incompatible-element-enriched lithospheric mantle. We believe that the amount, timing and distribution of magmatism in the Mahajanga basin were controlled by several factors, such as a hot thermal anomaly, lithosphere thickness and the composition and orientation of old tectonic lineaments. Geophysical studies of the crustal and lithospheric structure of Madagascar (Rambolamanana, Suhadolc & Panza, 1995; Rakotondraompiana, Albouy & Piqué, 1999; Piqué *et al.* 1999) suggest a relatively thick continental crust (30–42 km) below the Precambrian rocks in the centre of the island. A zone of substantially thinned crust is located below Antananarivo ($\approx$ 21 km) and along the eastern coast (25–27 km). E–W gravimetric profiles across Madagascar indicate that the lithosphere is thin beneath the Late Cenozoic volcanic fields of Ankaratra and Itasy (central Madagascar; Fig. 1) (Rakotondraompiana, Albouy & Piqué, 1999). A thick lithosphere ($\approx$ 130 km) is likely to be present beneath the eastern part of the island, whereas below the Karoo-related Morondava and Mahajanga basins, the lithosphere is likely to be thinner.

A simplified magmatic model proposed for the Mahajanga flood basalt sequence is illustrated in Figure 11. The essential components are: (1) the Archaean Antananarivo craton; (2) an incompatible-element-enriched lithospheric mantle source; (3) a depleted asthenospheric upper mantle source; and (4) a thermal anomaly. In this model a thermal anomaly only provides the heat to the adjacent mantle. In the western Mahajanga basin, decompression melting of a MORB-like mantle source generates the Antanimena magmas. These melts interact extensively during their
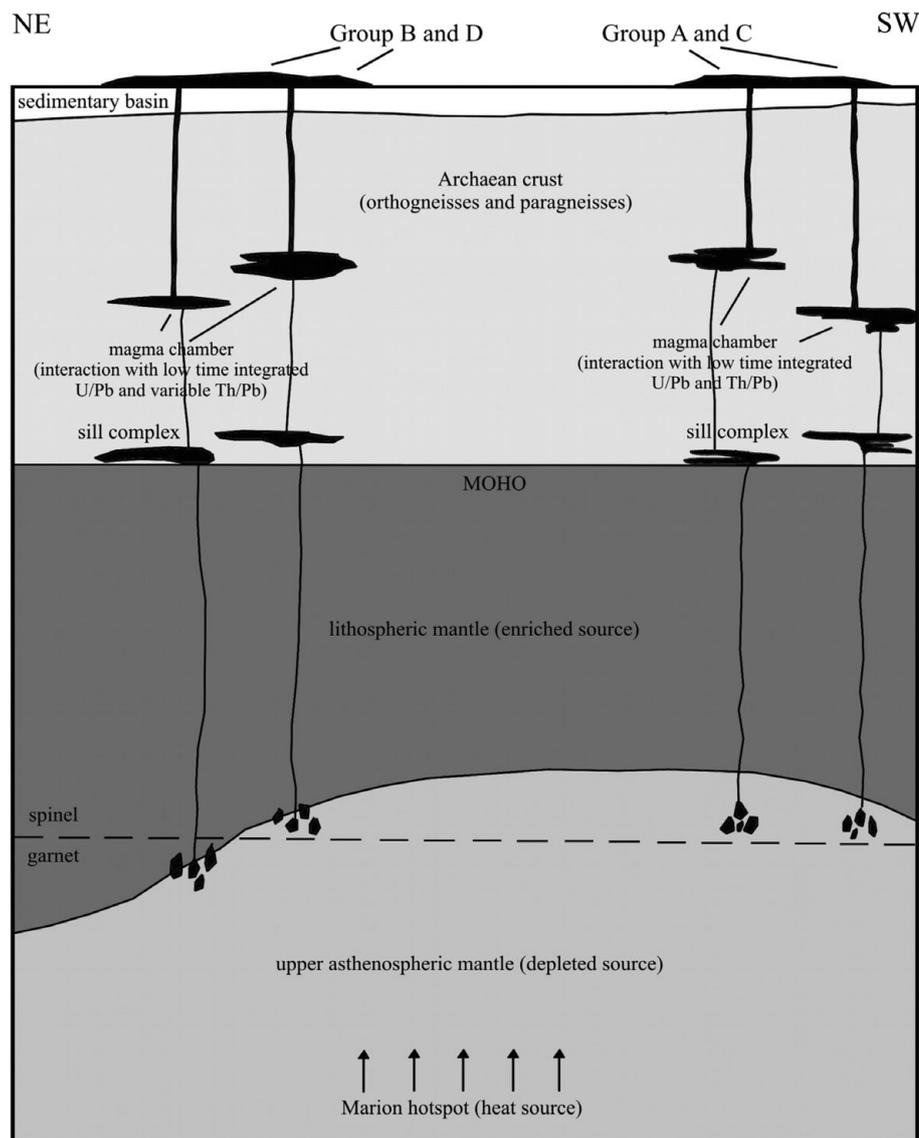
Figure 11. Model for the origin of the Mahajanga basalts. The figure is not to scale. The Antanimena rocks were generated by partial melting of a depleted upper asthenospheric mantle (heated by the Marion hotspot) and then contaminated with Archaean crustal material with low time-integrated U/Pb and Th/Pb. The Bongolava–Manasamody rocks were generated by mixing of melts from depleted upper asthenospheric mantle and enriched lithospheric mantle. These magmas were contaminated with Archaean crust with low U/Pb and variable Th/Pb ratios in crustal level magma chambers.

ascent with old crustal materials having very low Pb and Nd isotopes. In the eastern Mahajanga basin, depleted mantle-derived melts interact with melts derived from incompatible-element-enriched continental lithospheric mantle. Again, crustal-level contamination modifies the composition of the Group D magmas. An alternative hypothesis to explain the generation of the Mahajanga magmas without the involvement of the Marion hotspot requires small-scale convection in an internally heated upper mantle.

10. Conclusions

The new ^{40}Ar–^{39}Ar ages for plagioclase separates from basaltic rocks from the Antanimena plateau (western Mahajanga basin) constrain the beginning of the magmatism in this area at about 92 Ma and when combined with existing data, argue for a short emplacement duration. The lavas of the Mahajanga sector show distinct isotopic signatures. The Antanimena rocks are characterized by low Pb isotope ratios ($^{206}Pb/^{204}Pb$ = 15.283–16.325; $^{207}Pb/^{204}Pb$ = 15.058–15.269; $^{208}Pb/^{204}Pb$ = 35.483–36.547), whereas the Bongolava–Manasamody rocks are characterized by higher $^{206}Pb/^{204}Pb$ (16.518–17.355) and $^{208}Pb/^{204}Pb$ (37.511–38.009) but similar $^{207}Pb/^{204}Pb$ (15.086–15.404). The isotopic variations within the Mahajanga basalts and basaltic andesites are consistent with AFC processes involving different crustal end-members. The Pb isotopic compositions of the Antanimena rocks indicate that they have been contaminated by old continental crust with low time-integrated U/Pb and Th/Pb. In contrast, the higher $^{206}Pb/^{204}Pb$ and $^{208}Pb/^{204}Pb$ ratios observed in the Bongolava–Manasamody rocks (Group D) indicate a contaminant with higher time-integrated

U/Pb and Th/Pb. The Antanimena and Bongolava–Manasamody basalts cannot be related by variable degrees of partial melting of a common mantle source or by fractional crystallization of a common parental magma. The marked geochemical and isotopic differences between the Antanimena and Bongolava–Manasamody basalts indicate distinct mantle sources. The geochemical features of the Antanimena rocks show general affinities to normal MORB and indicate an incompatible-element-depleted mantle source. On the other hand, an incompatible-element-enriched mantle source is invoked to explain the geochemical features observed in the Bongolava–Manasamody rocks. The contribution of the Marion hotspot (as a magma source) to the northern part of the Madagascar Cretaceous province is not identifiable.

References

BAKSI, A. K. 2007*a*. A quantitative tool for evaluating alteration in undisturbed rocks and minerals – I: Water, chemical weathering and atmospheric argon. In *Plates, Plumes, and Planetary Processes* (eds G. R. Foulger & D. M. Jurdy), pp. 285–303. Geological Society of America, Special Publication no. 430.

BAKSI, A. K. 2007*b*. A quantitative tool for detecting alteration in undisturbed rocks and minerals – II: Application to argon ages related to hotspots. In *Plates, Plumes, and Planetary Processes* (eds G. R. Foulger & D. M. Jurdy), pp. 305–33. Geological Society of America, Special Publication no. 430.

BANKS, N., COOPER, B., JENKINS, S. & RAZAFINDRAKOTO, E. 2008. Evidence for the onshore extension of the deep water Jurassic salt basin in the Majunga Basin, northwest Madagascar. *Abstract, AAPG Annual Convention & Exhibition, San Antonio, Texas*.

BESAIRIE, H. 1964. *Geological map of Madagascar*. Tananarive: Service Géologique de Madagascar.

BESAIRIE, H. & COLLIGNON, M. 1972. Géologie de Madagascar I – Les terraines sédimentaires. *Annales Géologiques Madagascar* **35**, 553 pp.

BOYNTON, W. V. 1984. Cosmochemistry of the rare earth elements: meteorite studies. In *Rare Earth Element Geochemistry* (ed. P. Henderson), pp. 63–114. Amsterdam: Elsevier.

COLLINS, A. S. & WINDLEY, B. F. 2002. The tectonic evolution of central and northern Madagascar and its place in the final assembly of Gondwana. *Journal of Geology* **110**, 325–40.

CONDIE, K. C. 2005. TTGs and adakites: Are they both slab melts? *Lithos*, **80**, 33–44.

CREASER, R. A., PAPANASTASSIOU, D. A. & WASSERBURG, G. J. 1991. Negative thermal ion mass spectrometry of osmium, rhenium, and iridium. *Geochimica et Cosmochimica Acta* **55**, 397–401.

CUCCINIELLO, C., CONRAD, J., GRIFA, C., MELLUSO, L., MERCURIO, M., MORRA, V., TUCKER, R. D. & VIN-CENT, M. 2011. Petrology and geochemistry of Cretaceous mafic and silicic dykes and spatially associated lavas in central–eastern coastal Madagascar. In *Dyke Swarms: Keys for Geodynamic Interpretation* (ed. R. K. Srivastava), pp. 345–75. Berlin Heidelberg: Springer-Verlag.

CUCCINIELLO, C., LANGONE, A., MELLUSO, L., MORRA, V., MAHONEY, J. J., MEISEL, T. & TIEPOLO, M. 2010. U–Pb Ages, Pb–Os isotope ratios, and Platinum–Group Element (PGE) composition of the west–central Madagascar flood basalt province. *Journal of Geology* **118**, 523–41.

DALE, C. W., PEARSON, D. G., STARKEY, N. A., STUART, F. M., ELLAM, R. M., LARSEN, L. M., FITTON, J. G. & MACPHERSON, C. G. 2009. Osmium isotopes in Baffin Island and West Greenland picrites: implications for the $^{187}Os/^{188}Os$ composition of the convecting mantle and the nature of high He/He mantle. *Earth and Planetary Science Letters* **278**, 267–77.

DEPAOLO, D. J. 1981. Trace element and isotopic effects of combined wallrock assimilation and fractional crystallization. *Earth and Planetary Science Letters* **53**, 189–202.

DE WAELE, B., THOMAS, R. J., MACEY, P. H., HORSTWOOD, M. S. A., TUCKER, R. D., PITFIELD, P. E. J., SCHOFIELD, D. I., GOODENOUGH, K. M., BAUER, W., KEY, R. M., POTTER, C. J., ARMSTRONG, R. A., MILLER, J. A., RANDRIAMANANJARA, T., RALISON, V., RAFAHATELO, J.-M., RABARIMANANA, M. & BEJOMA, M. 2011. Provenance and tectonic significance of the Palaeoproterozoic metasedimentary successions of central and northern Madagascar. *Precambrian Research* **189**, 18–42.

DOSTAL, J., DUPUY, C., NICOLLET, C. & CANTAGREL, J. M. 1992. Geochemistry and petrogenesis of upper Cretaceous basaltic rocks from southern Madagascar. *Chemical Geology* **97**, 199–218.

DOWNES, H., MARKWICK, A. J. W., KEMPTON, P. D. & THIRLWALL, M. F. 2001. The lower crust beneath cratonic north-east Europe: isotopic constraints from garnet granulite xenoliths. *Terra Nova* **13**, 395–400.

ESCRIG, S., CAPMAS, F., DUPRÉ, B., ALLÈGRE, C.-J. 2004. Osmium isotopic constraints on the nature of the DUPAL anomaly from Indian mid–ocean–ridge basalts. *Nature* **431**, 59–63.

GRADSTEIN, F. M., OGG, J. G & SMITH, A. G. 2005. *A Geologic Time Scale 2004*. Cambridge: Cambridge University Press.

HART, S. R. 1984. A large-scale isotope anomaly in the southern Hemisphere mantle. *Nature* **309**, 753–7.

HOFMANN, C., FÉRAUD, G. & COURTILLOT, V. 2000. $^{40}Ar/^{39}Ar$ dating of mineral separates and whole rocks from the Western Ghats lava pile: further constraints on duration and age of the Deccan Traps. *Earth and Planetary Science Letters* **180**, 13–27.

JANNEY, P. E., LE ROEX, A. P. & CARLSON, R. W. 2005. Hafnium isotope and trace element constraints on the nature of mantle heterogeneity beneath the central Southwest Indian Ridge (13°E to 47°E). *Journal of Petrology* **46**, 2427–64.

JOURDAN, F., FÉRAUD, G., BERTRAND, H., WATKEYS, M. K. & RENNE, P. R. 2007. Distinct brief major events in the Karoo large igneous province clarified by new $^{40}Ar/^{39}Ar$ ages on the Lesotho basalts. *Lithos* **98**, 195–209.

KOPPERS, A. A. P. 2002. ArArCALC–software for $^{40}Ar/^{39}Ar$ age calculations. *Computers & Geosciences* **28**, 605–19.

KRAMERS, J. D. & TOLSTIKHIN, I. N. 1997. Two terrestrial lead isotope paradoxes, forward transport modelling,

core formation and the history of the continental crust. *Chemical Geology* **139**, 75–110.

KREISSIG, K., NAEGLER, T. F., KRAMERS, J. D., VAN REENEN, D. D. & SMIT, C. A. 2000. An isotopic and geochemical study of the northern Kaapvaal Craton and the Southern Marginal Zone of the Limpopo Belt: are they juxtaposed terranes? *Lithos* **50**, 1–25.

LYUBETSKAYA, T. & KORENAGA, J. 2007. Chemical composition of Earth's primitive mantle and its variance: 1 Method and results. *Journal of Geophysical Research*, **112**, 1–21.

MAHONEY, J. J., LE ROEX, A. P., PENG, Z. X., FISHER, R. L. & NATLAND, J. H. 1992. Southwestern limits of Indian Ocean ridge mantle and the origin of low $^{206}Pb/^{204}Pb$ MORB: isotope systematics of the central Southwest Indian Ridge (17°–50°E). *Journal of Geophysical Research* **97**, 19771–90.

MAHONEY, J. J., NATLAND, J. H., WHITE, W. M., POREDA, R., BLOOMER, S. H., FISHER, R. L. & BAXTER, A. N. 1989. Isotopic and chemical provinces of the western Indian ocean spreading centers. *Journal of Geophysical Research* **94**, 4033–52.

MAHONEY, J. J., NICOLLET, C. & DUPUY, C. 1991. Madagascar basalts: tracking oceanic and continental sources. *Earth and Planetary Science Letters* **104**, 350–63.

MAHONEY, J. J., SAUNDERS, A. D., STOREY, M. & RANDRIAMANANTENASOA, A. 2008. Geochemistry of the Volcan de l'Androy basalt – rhyolite complex, Madagascar Cretaceous igneous province. *Journal of Petrology* **49**, 1069–96.

MCBRIDE, J. S., LAMBERT, D. D., NICHOLLS, I. A. & PRICE, R. C. 2001. Osmium isotopic evidence for crust-mantle interaction in the genesis of continental intraplate basalts from the Newer Volcanics Province, Southeastern Australia. *Journal of Petrology* **42**, 1197–218.

MCDOUGALL, I. & HARRISON, T. M. 1999. *Geochronology and Thermochronology by the $^{40}Ar / ^{39}Ar$ Method*. Oxford: Oxford University Press, 269 pp.

MELLUSO, L., MORRA, V., BROTZU, P., D'ANTONIO, M. & BENNIO, L. 2002. Petrogenesis of the Late Cretaceous tholeiitic magmatism in the passive margins of northeastern Madagascar. In *Volcanic Rifted Margins* (eds M. A. Menzies, C. J. Ebinger & J. Baker), pp. 83–98. Geological Society of America, Special Paper no. 362.

MELLUSO, L., MORRA, V., BROTZU, P., FRANCIOSI, L., PETTERUTI LIEBERKNECHT, A. M. & BENNIO, L. 2003. Geochemical provinciality in the Cretaceous magmatism of northern Madagascar, and mantle source implications. *Journal of the Geological Society, London* **160**, 477–88.

MELLUSO, L., MORRA, V., BROTZU, P. & MAHONEY, J. J. 2001. The Cretaceous igneous province of Madagascar: geochemistry and petrogenesis of lavas and dykes from the central – western sector. *Journal of Petrology* **42**, 1249–78.

MELLUSO, L., MORRA, V., BROTZU, P., RAZAFINIPARANY, A., RATRIMO, V. & RAZAFIMAHATRATRA, D. 1997. Geochemistry and Sr–isotopic composition of the late Cretaceous flood basalt sequence of northern Madagascar: petrogenetic and geodynamic implications. *Journal of African Earth Sciences* **34**, 371–90.

MELLUSO, L., MORRA, V., BROTZU, P., TOMMASINI, S., RENNA, M. R., DUNCAN, R. A., FRANCIOSI, L. & D'AMELIO, F. 2005. Geochronology and petrogenesis of the Cretaceous Antampombato–Ambatovy complex and associated dyke swarm, Madagascar. *Journal of Petrology* **46**, 1963–96.

MELLUSO, L., MORRA, V. & FEDELE, L. 2006. An overview of phase chemistry and magmatic evolution in the Cretaceous flood basalt province of northern Madagascar. *Periodico di Mineralogia* **75**, 174–88.

MELLUSO, L., SHETH, H. C., MAHONEY, J. J., MORRA, V., PETRONE, C. M. & STOREY, M. 2009. Correlations between silicic volcanic rocks of the St. Mary's Islands (southwestern India) and eastern Madagascar: implications for Late Cretaceous India–Madagascar reconstructions. *Journal of the Geological Society, London* **166**, 1–12.

MEYZEN, C. M., LUDDEN, J. N., HUMLER, E., LUAIS, B., TOPLIS, M. J., MEVEL, C. & STOREY, M. 2005. New insights into the origin and distribution of DUPAL isotope anomaly in the Indian Ocean mantle from MORB of southwest Indian Ridge. *Geochemistry Geophysics Geosystems* **6**, Q11K11, doi:10.1029/2005GC000979.

MÖLLER, A., MEZGER, K. & SCHENK, V. 1998. Crustal age domains and the evolution of the continental crust in the Mozambique Belt of Tanzania: combined Sm–Nd, Rb–Sr and Pb–Pb isotopic evidence. *Journal of Petrology* **39**, 749–83.

NIU, Y & O'HARA, M. J. 2003. Origin of ocean island basalts: a new perspective from petrology, geochemistry and mineral physics considerations. *Journal of Geophysical Research* **108**, 2209, doi: 10.1029/2002JB002048.

NOMADE, S., KNIGHT, K. B., BEUTEL, E., RENNE, P. R., VERATI, C., FÉRAUD, G., MARZOLI, A., YOUBI, N. & BERTRAND, H. 2007. Chronology of the Central Atlantic Magmatic Province: implications for the Central Atlantic rifting processes and the Triassic–Jurassic biotic crisis. *Palaeogeography, Palaeoclimatology, Palaeoecology* **246**, 326–44.

PIQUÉ, A., LAVILLE, E., CHOTIN, P., CHOROWICZ, J., RAKOTONDRAOMPIANA, S. & THOUIN, C. 1999. L'extension à Madagascar du Néogène à l'Actuel: arguments structuraux et géophysiques. *Journal of African Earth Sciences* **28**, 975–83.

RAKOTONDRAOMPIANA, S., ALBOUY, Y. & PIQUÉ, A. 1999. Lithospheric model of the Madagascar island (western Indian Ocean): a new interpretation of the gravity data. *Journal of African Earth Sciences* **28**, 961–73.

RAMBOLAMANANA, G., SUHADOLC, P. & PANZA, G. F. 1995. Simultaneous inversion of hypocentral parameters and structural velocity of the central region of Madagascar as a premise for the mitigation of seismic hazard in Antananarivo. *International Centre for Theoretical Physics* **386**, Report IC/95, pp. 1–26.

RAZAFINDRAZAKA, Y., RANDRIAMANANJARA, T., PIQUE, A., THOUIN, C., LAVILLE, E., MALOD, J. & REHAULT, J.-P. 1999. Extension et sédimentation au Paléozoique terminal et au Mésozoïque dans le bassin de Majunga (Nerd–Ouest de Madagascar). *Journal of African Earth Sciences* **28**, 949–59.

REISBERG, L., LORAND, J.-P. & BEDINI, R. M. 2004. Reliability of Os model ages in pervasively metasomatized continental mantle lithosphere: a case study of Sidamo spinel peridotite xenoliths (East African Rift, Ethiopia). *Chemical Geology* **208**, 119–40.

RENNE, P. R., MUNDIL, R., BALCO, G., MIN, K. & LUDWIG, K. R. 2010. Joint determination of ^{40}K decay constants and $^{40}Ar*/^{40}K$ for the Fish Canyon sanidine standard, and improved accuracy for $^{40}Ar/^{39}Ar$ geochronology. *Geochimica et Cosmochimica Acta* **74**, 5349–67.

RENNE, P. R., SWISHER, C. C., DEINO, A. L., KARNER, D. B., OWENS, T. & DEPAOLO, D. J. 1998. Intercalibration of

standards, absolute ages and uncertainties in $^{40}Ar/^{39}Ar$ dating. *Chemical Geology* **145**, 117–52.

ROY-BARMAN, M. 1993. Mesure du rapport $^{187}Os/^{188}Os$ dans le basaltes et péridotites: contribution à la systématique ^{187}Re-^{187}Os dans le manteau. Ph.D. thesis, University of Paris VII, Paris, France. Published thesis.

RUDNICK, R. L. & GAO, S. 2003. Composition of the continental crust. In *The Crust* (ed. R. L. Rudnick), pp. 1–64. Treatise on Geochemistry vol. 3. Amsterdam: Elsevier.

SAAL, A. E., RUDNICK, R. L., RAVIZZA, G. E. & HART, S. R. 1998. Re–Os isotope evidence for the composition, formation and age of the lower continental crust. *Nature* **393**, 58–61.

SENGUPTA, S., PAUL, D. K., DE LAETER, J. R., MCNAUGHTON, N. J., BANDOPADHYAY, P. K., DE SMETH, J. B. 1991. Mid-Archean evolution of the Eastern Indian Craton: geochemical and isotopic evidence from the Bonai pluton. *Precambrian Research* **49**, 23–37.

SHIREY, S. B. & WALKER, R. J. 1995. Carius tube digestion for low blank rhenium- osmium analysis. *Analytical Chemistry* **67**, 2136–41.

SHIREY, S. B. & WALKER, R. J. 1998. The Re–Os isotope system in cosmochemistry and high-temperature geochemistry. *Annual Review of Earth and Planetary Sciences* **26**, 423–500.

SIMON, N. S., CARLSON, R. W., GRAHAM PEARSON, D. & DAVIES, G. R. 2007. The origin and evolution of the Kaapvaal cratonic lithospheric mantle. *Journal of Petrology* **48**, 589–625.

SIMON, J. I., RENNE, P. R. & MUNDIL, R. 2008. Implications of pre-eruptive magmatic histories of zircons for U–Pb geochronology of silicic extrusions. *Earth and Planetary Science Letters* **266**, 182–94.

STEIGER, R. H. & JÄGER, E. 1977. Subcommission on geochronology: convention on the use of decay constants in geo- and cosmochronology. *Earth and Planetary Science Letters* **36**, 359–62.

STERN, R. J. 1994. Arc assembly and continental collision in the Neoproterozoic East African Orogeny–implications for the consolidation of Gondwana. *Annual Review of Earth Planetary Sciences* **22**, 319–51.

STOREY, M., MAHONEY, J. J. & SAUNDERS, A. D. 1997. Cretaceous basalts in Madagascar and the transition between plume and continental lithosphere mantle sources. In *Large Igneous Provinces: Continental, Oceanic and Planetary Flood Volcanism* (eds J. J. Mahoney & M. F. Coffin), pp. 95–122. American Geophysical Union, Geophysical Monograph vol. 100. Washington, DC, USA.

STOREY, M., MAHONEY, J. J., SAUNDERS, A. D., DUNCAN, R. A., KELLEY, S. P. & COFFIN, M. F. 1995. Timing of hot spot-related volcanism and the breakup of Madagascar and India. *Science* **267**, 852–5.

TODT, W., CLIFF, R. A., HANSER, A. & HOFMANN, A. W. 1996. Evaluation of a ^{202}Pb-^{205}Pb double spike for high-precision lead isotopic analyses. In *Earth Processes: Reading the Isotopic Code* (eds A. Basu & S. R. Hart), pp. 429–37. American Geophysical Union, Geophysical Monograph vol. 95. Washington, DC, USA.

TORSVIK, T. H., TUCKER, R. D., ASHWAL, L. D., EIDE, E. A., RAKOTOSOLOFO, N. A. & DE WIT, M. J. 1998. Late Cretaceous magmatism of Madagascar: paleomagnetic evidence for a stationary hotspot. *Earth and Planetary Science Letters* **164**, 221–32.

TUCKER, R. D., ASHWAL, L. D., HANDKE, M. J., HAMILTON, M. A., LE GRANGE, M. & RAMBELOSON, R. A. 1999. U–Pb geochronology and isotope geochemistry of the Archean and Proterozoic rocks of north-central Madagascar. *Journal of Geology* **107**, 135–53.

VÖLKENING, J., WALCZYK, T. & HEUMANN, K. G. 1991. Osmium isotope ratio determinations by negative thermal ionization mass spectrometry. *International Journal of Mass Spectrometry and Ion Processes* **105**, 147–59.

WALKER, R. J., CARLSON, R. W., SHIREY, S. B. & BOYD, F. R. 1989. Os, Sr, Nd, and Pb isotope systematics of southern African peridotite xenoliths: implications for the chemical evolution of subcontinental mantle. *Geochimica et Cosmochimica Acta* **53**, 1583–95.

WALKER, R. J. & MORGAN, J. W. 1989. Rhenium-osmium isotope systematics in carbonaceous chondrites. *Science* **243**, 519–22.

XU, J.-F., SUZUKI, K., XU, Y.-G., MEI, H. J. & LI, J. 2007. Os, Pb, and Nd isotope geochemistry of the Permian Emeishan continental flood basalts: insights into the source of a large igneous province. *Geochimica et Cosmochimica Acta* **71**, 2104–19.

Appendix 1. Analytical methods

Eleven samples from the Mahajanga basin were selected for isotope analyses. These samples represent the different magma types identified by Melluso *et al*. (1997, 2003). Lead isotopic data were obtained at the School of Ocean and Earth Sciences and Technology, University of Hawaii, following Mahoney, Nicollet & Dupuy (1991) and Mahoney *et al*. (1992). Crushed chips were acid-cleaned in 0.15 mol l^{-1} HF-HNO$_3$ for 5 minutes (in an ultrasonic bath) and dissolved successively in concentrated HF-HNO$_3$, HNO$_3$, and HCl. A split of each solution was spiked with ^{206}Pb. Lead was subsequently separated and purified on 100-μl anion exchange columns with mixed HBr-HNO$_3$ concentrated solutions. The lead-bearing fraction was loaded onto single Re filaments with concentrated H_3PO_4 and silica-gel, and isotopic ratios were measured on a VG Sector multicollector thermal ionization mass spectrometer. Lead isotope ratios are corrected for fractionation using the NBS 981 standard values of Todt *et al*. (1996). The blank contribution to the measurement result was negligible (< 19 pg).

Rhenium and osmium analyses were performed on whole rocks, following Reisberg, Lorand & Bedini (2004). About 2 g of sample powder were spiked with ^{185}Re and ^{190}Os tracer solutions and digested in a Carius tube (Shirey & Walker, 1995) at 230 °C using a 3:1 mixture of HNO$_3$ and HCl. Carius tubes (CT) are thick-walled, sealed borosilicate glass tubes, meant to withstand high pressures, that permit samples to be digested in oxidizing solutions without loss of the volatile species, OsO$_4$. After purification of the separated Os by microdistillation (Roy-Barman, 1993), Os isotopic ratios were measured by negative thermal ionization (Creaser, Papanastassiou & Wasserburg, 1991; Völkening, Walczyk & Heumann, 1991) in ion counting mode using a Finnigan MAT262 mass spectrometer at CRPG (Centre National de la Recherche Scientifique–Centre de Recherches Pétrographiques et Géochimiques). Os concentrations were determined by isotope dilution (ID). The average total procedural blank for Os was 1.3 ± 0.7 pg. The $^{187}Os/^{188}Os$ ratio of in-house reference materials had a precision under intermediate precision conditions of 0.3 % (0.17386 ± 0.00054; 2σ; n = 45) during one year. The measurement uncertainties of single concentration determinations of Os were about 1 % or less. However, repeated analysis of samples leads to higher uncertainties due to the heterogeneous distribution of Re and Os. The differences in isotopic composition and Re and Os content exceed the uncertainties by far, thus the contribution from

sample inhomogeneity was not further investigated by repeated analysis.

The solution aliquot saved for Re separation was dried down and redissolved in 0.4 N HNO_3. Re was extracted from this solution using AG1×8 anion exchange resin columns. Spiked Re isotopic ratios were determined by peak jumping using a Daly detector on a Micromass Isoprobe MC-ICP-MS, and Re concentrations were calculated by ID. Mass fractionation was controlled by standard measurements taken after every four samples. The isotope amount ratio $^{187}Re/^{185}Re$ normally varied by $\sim$ 0.3 % throughout the course of a day. Total procedural blanks of Re were about 4 pg.

We selected two samples from the base of the Antanimena plateau that showed few signs of alteration (M420 and M422) for ^{40}Ar–^{39}Ar dating and separated unaltered, optically transparent plagioclase from them. Plagioclase was separated using a Frantz magnetic separator, and carefully hand-picked under a binocular microscope. The selected grains were then leached in dilute HF for one minute and then thoroughly rinsed with distilled water in an ultrasonic cleaner. Samples were loaded into two large wells of an aluminium disc. The wells were 1.9 cm in diameter and 0.3 cm in depth. These wells were bracketed by small wells that included GA1550 biotite used as a neutron fluence monitor, for which an age of 98.79 $\pm$ 0.55 Ma was adopted at the time of the measurement and a good in between grain reproducibility has been demonstrated (Renne et al. 1998). The discs were Cd-shielded (to minimize undesirable nuclear interference reactions) and irradiated for 25 hours in the Hamilton McMaster University (Canada) nuclear reactor. The mean J-values computed from standard grains within the small pits range from 0.007054 ($\pm$ 0.21 %) to 0.006880 ($\pm$ 0.34 %) determined as the average and standard deviation of J-values of the small wells for each irradiation disc. Mass discrimination was monitored using an automated air pipette and provided mean values ranging from 1.001286 ($\pm$ 0.36 %) to 1.001553 ($\pm$ 0.30 %) per dalton (atomic mass unit). The correction factors for interfering isotopes were $(^{39}Ar/^{37}Ar)_{Ca}$ = 7.30 × 10^{-4} ($\pm$ 11 %), $(^{36}Ar/^{37}Ar)_{Ca}$ = 2.82 × 10^{-4} ($\pm$ 1 %) and $(^{40}Ar/^{39}Ar)_K$ = 6.76 × 10^{-4} ($\pm$ 32 %).

The ^{40}Ar–^{39}Ar analyses were performed at the Western Australian Argon Isotope Facility at Curtin University. The samples were loaded in 0-blank Cu-foil packages and were step heated using a Pond Engineering® double vacuum resistance furnace. The gas was purified in a stainless steel extraction line using a GP50 and two AP10 SAES getters and a liquid nitrogen condensation trap. Argon isotopes were measured in static mode using a MAP 215–50 mass spectrometer (resolution of $\sim$ 500; sensitivity of 2 × 10^{-14} mol V^{-1}) with a Balzers SEV 217 electron multiplier, mostly using nine to ten cycles of peak-hopping. Data acquisition was performed with the Argus program written by M. O. McWilliams; the program ran in a LabView environment. The raw data were processed using the ArArCALC software (Koppers, 2002). Argon isotopic data corrected for blank, mass discrimination and radioactive decay are given in Table 1. Individual errors in Table 1 are given at the 1σ level. Initially, the ages were obtained and calculated using the decay constants recommended by Steiger & Jäger (1977) but plateau and isochron ages were subsequently individually recalculated using the new decay constants determined by Renne et al. (2010) and an age of 99.769 $\pm$ 0.108 Ma ($\pm$ 0.11 %) Ma for GA1550. Recalculated values are shown in Table 2. Uncertainties on the plateau and isochron ages include all sources of errors, including error on the decay constant and uncertainty on the age of the monitor. Blanks were monitored every three to four steps and typical ^{40}Ar blanks ranged from 1 × 10^{-16} to 2 × 10^{-16} mol. Our criteria for the determination of a plateau are as follows: plateaus must include at least 70 % of the ^{39}Ar, and a plateau should be distributed over a minimum of three consecutive steps agreeing at the 95 % confidence level and satisfying a probability of fit (P) of at least 0.05. Plateau ages (Table 2 and Fig. 5) are given at the 2σ level and are calculated using the mean of all the plateau steps, each weighted by the inverse variance of the individual analytical error. Integrated ages (2σ) are calculated using the total gas released for each Ar isotope. Inverse isochrons include the maximum number of steps with a probability of fit $\geq$ 0.05.